Review of soft fluidic actuators: classification and materials modeling analysis

Amir Pagoli, Frédéric Chapelle, Juan Antonio Corrales Ramon, Youcef Mezouar, Yuri Lapusta

Review of soft fluidic actuators: classification and materials modeling analysis

OPEN ACCESS
IOP Publishing
Smart Materials and Structures
Smart Mater. Struct. **31** (2022) 013001 (30pp)
https://doi.org/10.1088/1361-665X/ac383a

Topical Review

Review of soft fluidic actuators: classification and materials modeling analysis

Amir Pagoli[1,*], Frédéric Chapelle[1], Juan-Antonio Corrales-Ramon[2], Youcef Mezouar[1] and Yuri Lapusta[1]

[1] Université Clermont Auvergne, Clermont Auvergne INP, CNRS, Institut Pascal, Clermont-Ferrand, F-63000, France
[2] CiTIUS (Centro Singular de Investigación en Tecnoloxías Intelixentes), Universidade de Santiago de Compostela, 15782 Santiago de Compostela, Spain

E-mail: amir.pagoli@sigma-clermont.fr

Received 7 February 2021, revised 6 June 2021
Accepted for publication 10 November 2021
Published 7 December 2021

Abstract

Soft actuators can be classified into five categories: tendon-driven actuators, electroactive polymers, shape-memory materials, soft fluidic actuators (SFAs), and hybrid actuators. The characteristics and potential challenges of each class are explained at the beginning of this review. Furthermore, recent advances especially focusing on SFAs are illustrated. There are already some impressive SFA designs to be found in the literature, constituting a fundamental basis for design and inspiration. The goal of this review is to address the latest innovative designs for SFAs and their challenges and improvements with respect to previous generations, and to help researchers to select appropriate materials for their application. We suggest seven influential designs: pneumatic artificial muscle, PneuNet, continuum arm, universal granular gripper, origami soft structure, vacuum-actuated muscle-inspired pneumatic, and hydraulically amplified self-healing electrostatic. The hybrid design of SFAs for improved functionality and shape controllability is also considered. Modeling SFAs, based on previous research, can be classified into three main groups: analytical methods, numerical methods, and model-free methods. We demonstrate the latest advances and potential challenges in each category. Regarding the fact that the performance of soft actuators is dependent on material selection, we then focus on the behaviors and mechanical properties of the various types of silicone that can be found in the SFA literature. For a better comparison of the different constitutive models of silicone materials proposed and tested in the literature, ABAQUS software is here employed to generate the engineering and true strain-stress data from the constitutive models, and compare them with standard uniaxial tensile test data based on ASTM412. Although the figures presented show that in a small range of stress–strain data, most of these models can predict the material model acceptably, few of them predict it accurately for large

* Author to whom any correspondence should be addressed.

strain-stress values. Sensor technology integrated into SFAs is also being developed, and has the potential to increase controllability and observability by detecting a wide variety of data such as curvature, tactile contacts, produced force, and pressure values.

Keywords: soft robotics, fluidic elastomer actuators, constitutive models, soft materials, FEM analysis

(Some figures may appear in colour only in the online journal)

1. Introduction

For many decades, scientists have tried to bring their robot designs closer to human body performances. Advances in materials and soft components are expanding the range of new types of robots that perform complex tasks and interact more closely with humans. They have pushed back the boundaries in the field of robotics with their remarkable capabilities, including lightweight, hyper redundancy, fast assembly and cost-effective materials [1]. Furthermore, soft robots can be actuated using different strategies, such as pneumatic or hydraulic fluids, electric motors, heat, chemical reactions, etc [2]. Unlike soft robots, conventional robots are rigid and consist of a number of links connected together by joints; they are designed to work in specific environments and satisfy recurrent high-precision tasks. Although these manipulators are very common in many industries such as automotive and food, they have some limitations, such as limited dexterity and an insufficient number of degrees of freedom (DOFs). These limitations restrict their movements in arbitrary workspaces. Inspired by nature, soft robots have emerged and reduced the gap between human interaction and robotic environments. Additionally, they provide interesting new capacities in comparison with other robotic architectures; for instance, soft robots are capable of maneuvering through congested environments with minimum inducing stress concentrations or damage.

Many classification approaches have been used to characterize satisfactorily their structures and performances. Trivedi *et al* divided robots into two classes, according to their materials and DOFs: soft and hard robots [3]. Soft robots were categorized as a subset of continuum robots. This means that soft robots are able to act with continuous deformation, but not all continuum robots are soft. For instance, some of them include several hard links and joints, creating more DOFs. A number of DOFs largely higher than the number of actuators puts them in the hyper redundant robot class. Although many DOFs are not controllable, they increase the shape configuration adaptability of a robot with various objects. Several reviews on soft robots have been carried out and can be found in the literature; most of them are focused on the recent advances in this field [4–9]. Shintake *et al* [10] classified soft grippers in three separate groups based on their grasping technology: actuation, adhesion control and variable stiffness control. Boyraz *et al* [2] presented a comprehensive comparison of soft robot actuators and mentioned their challenges. Gorissen *et al* [11] and Walker *et al* [12] separately reviewed the design, manufacturing and control of soft pneumatic actuators. They focused on soft pneumatic actuators with positive pressure, while soft fluidic actuators (SFAs) with negative pressure play a significant role in achieving soft robot milestones. In this study, we classify soft robots based on their actuation mechanism into five classes: 1—tendon-driven actuation, 2—electroactive polymers (EAPs): dielectric elastomer actuators (DEAs) and ionic polymer-metal composites (IPMCs), 3—shape-memory materials: shape memory alloys (SMAs) and shape memory polymers (SMPs), 4—SFAs (see figure 1), 5—hybrid actuators. Although additional soft actuators such as a soft magnetic robot [13], soft grippers using gecko-adhesion [14], fishing line actuator [15], electrorheological fluids [16], and magnetorheological fluids [17] are reported in the literature, due to their rare usage, in this study, we have focused on reviewing these five mentioned classes of soft actuators.

We first position SFAs in relation to other soft actuation technologies, then we suggest a general classification of the SFA domain by considering all pressurized and vacuum technologies. We then summarize the most effective SFA designs that could be a source of inspiration for future approaches. Furthermore, SFA functions are strongly dependent on the type and properties of the selected material. Silicone is the most commonly-used material in SFAs. Due to its highly nonlinear behavior, modeling and operating prediction are the main challenging aspects of SFAs. In this paper, we study a wide variety of silicones and review the different modeling methods.

2. Soft actuation technologies and SFAs

As mentioned, this review paper is focused on SFAs as one of the most common actuation mechanisms in the field of soft robots, but it is necessary to explain briefly the other actuation methods to help to clarify the reason for choosing SFAs to review as one of the soft robot actuator approaches. Moreover, in hybrid designs, SFAs can be integrated with other actuation types to enhance robot performance. Figure 1 shows the most representative actuator technologies in soft robots based on previously published results. The major advantages and challenges of each actuation method are summarized in table 1 and explained in the remaining part of this section.

The first category concerns tendon-driven actuation. It is widely used in continuum soft robots. This technology enables them to reach the desired position with many different configurations, so they have high dexterity and superior performance in congested environments [15, 24, 50 51]. In a continuum soft robot, a moment is applied at the tip of the arm with the tendon mechanism, then the whole arm deforms

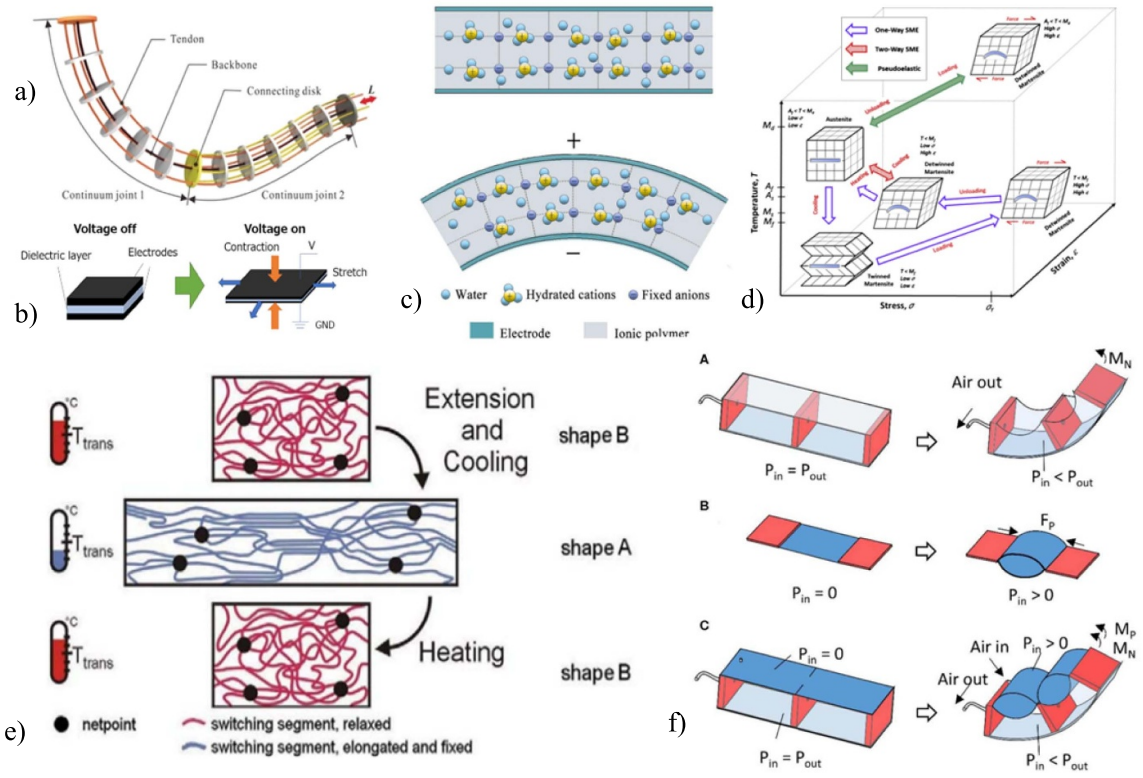

Figure 1. Different types of actuation in soft robots. (a) Tendon-driven mechanisms. Reproduced from [18]. (b) Dielectric elastomer actuators (DEAs). Reproduced from [19]. CC BY 4.0. (c) Ionic polymer-metal composites (IPMCs) Reproduced from [20]. CC BY 4.0. (d) Shape memory alloys (SMAs). Reprinted from [21], (e) Shape memory polymers (SMPs). Reproduced from [22] (f) Soft fluidic actuators (SFAs). Reproduced from [23]. CC BY 4.0.

Table 1. Different type of soft robot actuators.

Design parameters	Power supply	Advantages	Challenges
Tendon driven mechanisms	Electric motor	Large stroke bending with a high produced force	Require external motors
Dielectric elastomer actuators (DEAs)	Electric	Large actuation strokes, self-sensing capability, fast response time, requiring small currents	Require high voltages; difficult fabrication procedure for complex geometry
Ionic polymer-metal composites (IPMCs)	Electric	Bending in both directions, variable stiffness, large bending strokes with low actuation voltages, self-sensing	Slow response and low produced force
Shape memory alloys (SMAs)	Electric or thermal	High active stress, high elastic modulus, conductivity without the need for an external heater, act as a strain sensor at the same time	Slow response and speed, hysteresis, require high currents
Shape memory polymers (SMPs)	Thermal or electric	Variable stiffness capability	Low produced force
Fluidic actuators	Pneumatic or hydraulic	High force generation, large stroke bending	Require external pumps, bulky and heavy

smoothly and continuously (figure 1(a)). It can transmit compressive forces, which enabling it to perform perfectly in complex conditions or when encountering obstacles. Due to their inherent design, continuum robots can grasp objects by using whole arm manipulation, and carry payloads without causing damage. Recently, a variety of actuators, joints, and mechanisms inspired by nature have been built, such as those connecting several small links [52], Serpentine Robot [53], and elephant trunks with a single flexible backbone actuated by wires [54]. Xu and Simaan designed human body surgery

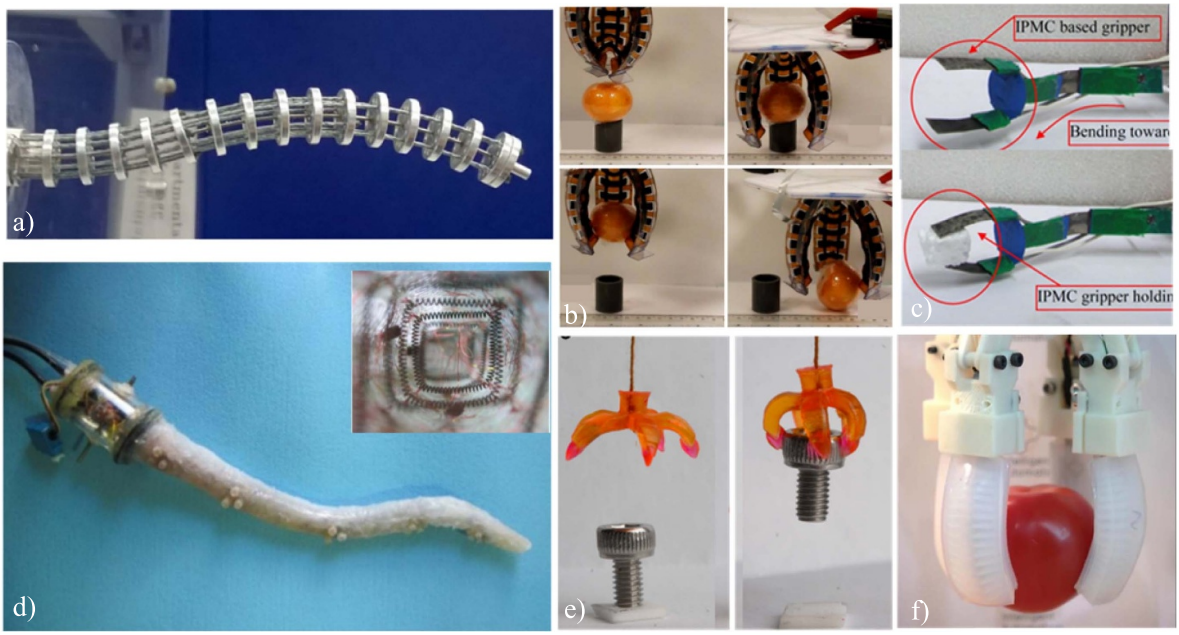

Figure 2. Examples of different actuation types in the soft robotics field: (a) surgery robot using a tendon-driven mechanism. Reproduced from [25]. CC BY 4.0. (b) DEA soft gripper. Reproduced with permission from [37]. (c) IPMC gripper for manipulating the object Reproduced from [46]. CC BY 4.0. (d) SMA spring soft actuator Reproduced from [47]. CC BY 4.0. (e) SMP soft gripper. Reproduced from [48]. CC BY 4.0. (f) Soft pneumatic actuator. Reproduced from [49] CC BY 4.0.

robots with multiple flexible backbones actuated in push-pull mode [55], applicable for tele-operated surgery in the throat and upper airways [56]. Figure 2(a) shows the snake-like robot design by Ouyang *et al* [25]. This design is composed of a base disk, an end disk, several spacer disks, and four arranged super-elastic NiTi tubes. The central tube is the primary backbone, while the remaining three tubes are the secondary backbones. By pulling two of these three secondary backbones in each section and changing their lengths, the end disk can be oriented in any required direction in space. To study more about the other types of tendon-driven soft robots, the reader may refer to [3, 26, 57]. The second class of soft robot actuators is EAPs. They respond to electrical stimulation with significant changes in dimension or shape [27]. DEAs and IPMCs are the two most well-known EAP technologies, especially in the robotics field [28, 58–60]. DEAs consist of a thin elastomer membrane between two compliant electrodes (figure 1(b)) [19]. By applying a voltage, the elastomer starts to deform, and consequently mechanical actuation appears [61]. The main performance advantages of DEAs can be highlighted by large deformation [62], high energy density, fast responses [29], lightweight and low cost [30]. Moreover, DEAs self-sensing [31, 32] and variable-shape configuration capabilities make them a wise choice in soft robotic actuators [33, 34]. Anderson *et al* [35] reviewed DEA applications as artificial muscle to generate many translational and rotational DOFs, especially for soft machines. The DEAs' multifunctionality in actuation and sensing capability provide feedback control in the closed-loop system without requiring any external sensor. In addition, they remarked the most important self-sensing potential factors in DEAs, namely material development, reliability, manufacturability, and miniaturizing. Araromi *et al* [36] proposed a small-scale gripper consisting of a pre-stretched elastomer DEA actuator. By applying a voltage, the 0.65 g gripper can bend up to 60 degrees and produce a 2.2 mN gripping force. As shown in figure 2(b), a stiff layer of polyvinyl chloride sheet can be added to DEA elastomer [37]. This layer increases the generated grasping force to 168 mN. The potential challenge of DEAs is that they require high voltages in the kV range, which not only raises the cost and size of the kV control electronics but also increases the risk of electrical discharge, undesirable in many applications, especially with human interaction [38–40]. A potential solution to this problem is decreasing the dielectric membrane thickness. The optimum range of DEA thickness is between 20 and 100 μm, whereby reducing more than this range increases fabrication challenge [41]. Ji *et al* [42] presented low-voltage stacked DEAs with an operating voltage below 450 volts to fabricate an ultralight (1 g) insect-sized (40 mm long), and fast (30 mm s^{-1} tethered, 12 mm s^{-1} untethered) device. Moreover, the operating voltage of DEAs can also be decreased by increasing the elastomer permittivity [43, 44] or reducing the elastic modulus [45]. Gu *et al* reviewed recent works in the DEA-driven soft robot field; they tried to summarize the challenges and opportunities for further mechanism design, dynamics modeling and autonomous control [63].

Hydraulically amplified self-healing electrostatic (HASEL) is a similar mechanism to DAE which has been advanced recently by Acome *et al* [64]. Like DEA, HASEL actuators include two flexible layers but use liquid dielectric instead of elastomers. The electric field applies electrostatic force

to drive shape change in a soft fluidic architecture by transporting fluid through a system of channels. Unlike DEAs, HASEL actuators are fabricated without a pre-stretch layer or rigid frames, making them suitable for building soft actuators [65]. Moreover, liquid dielectric provides an electrically self-healing capability in the event of a dielectric breakdown. As a result, HASEL actuators generate large strains and fast response while having self-sensing capabilities, especially for developing closed-loop control of soft robots [66]. However, the potential challenges of HASEL actuators similar to DEA, for achieving fats response required very high voltages (≈20 kV). Besides, for sealing fabrication of the elastomers for the layers, two standard molding cast or metal die methods are used, which are time-consuming processes for different geometries and designs [67]. Recent techniques have focused on miniaturizing high-voltage dc-dc converters as a promising solution for both HASEL and DEA actuation [68]. The XP Power and Pico Electronics are two famous commercial converters that can produce up to 10 kV using a 5 V input [69]. Although the functionality of the HASEL actuators is more similar to the DEAs, due to the pressurizing the fluid, some applications with HASEL can be classified as a soft pressurized fluidic actuator (SPFA). More details about these types of actuators in soft robots are explained in the corresponding section.

Another widespread type of EAP material is IPMC, which bends in response to electrical activation [70]. A typical IPMC consists of chemically-plated gold or platinum on a perfluoro sulfonic acid membrane, which is known as an ion-exchange membrane. When an input voltage is applied to the metal layers, the cations move toward the cathode. This translation generates strain and the IPMC starts to bend toward the anode [20] (figure 1(c)). Shahinpoor *et al* [71] classified their IPMC study in a series of four reviews to present a summary of the fundamental properties and characteristics: various techniques and experimental procedures in manufacturing [72], modeling and simulation analysis [73], and finally industrial and medical applications for IPMC [74]. Due to several advantages, including a low activation voltage ($1 \sim 3$ V), self-sensing capability, ease of miniaturization, and operation in wet conditions, IPMC technology has been used in actuators and sensors in soft robotics for the last two decades. Kashmery [46] fabricated grippers composed of an IPMC membrane actuator to manipulate a small object by applying 5 V DC (figure 2(c)). Slow actuator response and low produced stress are the most challenging issues when using IPMC as an actuator [10]. Recent technologies and applications of IPMCs are reviewed in [75–77]. Hao *et al* reviewed the latest advances in IPMCs for soft actuators and sensors, especially in the field of soft robotics [78].

Shape memory materials are another actuation method widely used in soft robotics, due to their deformation in response to electrical stimuli or temperature. SMAs and SMPs are the two kinds of materials which exhibit these characteristics. Figure 1(d) shows the two well-known properties of SMAs. The first is the phenomenon of phase transformation between martensite and austenite, which leads to mechanical actuation and subsequent return to their original shape [79]. The second feature of SMAs is the superelastic effect, which is the ability of the material to recover its large elastic deformations upon removal of the load [80]. As is the case for tendon-driven actuation, this second property of SMAs is widely used in continuum robots to push/pull cables. This kind of SMA is a nickel-titanium alloy known as Nickel-titanium. The amount of deformation and stroke produced during a heating/cooling cycle is depended on the shape of the SMA and its thermomechanical treatment. Nowadays, the use of SMAs as actuators in soft robots is growing because of the promising advantages of being able to significantly reduce actuator size, the available rapid manufacturing techniques, the large actuation force, and the displacement. Cianchetti *et al* [47] designed soft actuators with a combination of SMA springs and braided sleeves for multi-purpose applications in water (figure 2(d)). The conductivity features of SMAs enable them to utilize the direct Joule heating technique without needing an external heater [81]. However, the potential challenges of using SMAs as actuators remain; for instance, their slow operation frequency, controllability, accuracy, energy efficiency, and recovery speed are important issues [21].

SMPs are considered as memorized polymers that can change shape under heat or light stimulation and transform from a temporary shape to a memorized permanent shape [82, 83] (figure 1(e)). Because of low recovery speed and hysteresis, few works can be found using SMPs as the main actuators of soft robots [84]. Figure 2(e) shows a SMP small-scale gripper with four fingers. The gripper can hold small objects such as a screw after heat actuation [48]. SMPs are usually integrated into other technologies such as SMAs [85] and SFAs [86] to vary the stiffness of the robot. These hybrid mechanisms will be discussed in more detail in the dedicated section. Recent progress on SMPs and their potential challenges are reviewed in [83–89].

The SFA is one of the most ubiquitous actuation mechanisms in soft robotics due to its many advantages, including simple assembly, cost-effective materials, large deformation, and high generated force [23, 90] (figure 1(f)). These unique characteristics make them promising candidates for various applications, such as gripping [10, 91–93], mobility [94], robotic manipulation [95–97] medical applications [98, 99], and rehabilitation and assistive robotics [100, 101]. By applying positive or negative pressure inside the chamber, the soft actuator, depending on the type of surface where the pressure is applied, starts to bend, extend, twist, or contract [49, 102] (figure 2(f)). Moreover, in hybrid designs SFAs can be integrated with other actuation types to enhance robot performance [2].

As seen in this section, each actuation strategy has some capability which differs drastically in terms of performance from the others, such as response speed, stroke, amount of force produced, and variable stiffness. SFAs have particularly wide application areas and are reported frequently [103]. Due to the huge potential of SFAs, we focus in this review paper on some of the developments in their various applications in soft robotics and discuss the recent progress of soft robots

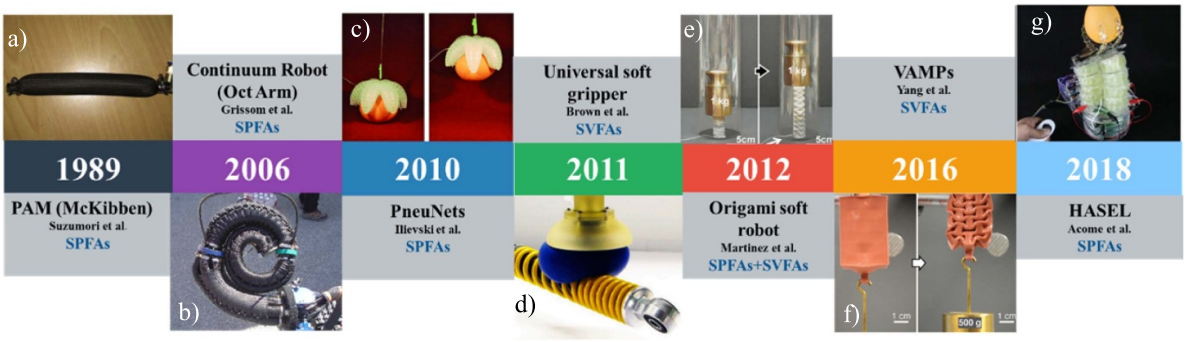

Figure 3. Timeline showing major production advances in the field of SFAs: (a) PAM mechanism developed by Suzumuri *et al* [104] (Reprinted from Xing *et al* [105]). (b) OctArm. Reproduced with permission from [106]. (c) PneuNets. Reproduced from [107]. (d) Universal gripper. Reproduced with permission from [108]. (e) Origami soft structure [109] VAMPs design. Reproduced from [110], and (g) HASEL actuator [64] Reproduced from Mitchell *et al* [111]. CC BY 4.0.

using SFAs. In the following sections we review recent developments in the field of SFA regarding classification, design, computational procedures, and the history of the most effective SFAs design mechanisms which have inspired many works over the last two decades.

3. History and classification of SFAs

We classify SFAs based on the applied pressure in three mains categories: SPFAs, soft vacuumed fluid actuators (SVFAs), and hybrid mechanisms including a combination of SFA with the other existing types of soft actuators explained in the soft actuation section. In SPFAs, positive pressure is used to inflate channels in a soft material and cause the desired deformation, while in SVFAs, vacuuming the air inside the chamber causes contraction. We review the most significant research based on these three categories. Figure 3 shows the timeline.

3.1. Soft pressurized fluidic actuators (SPFAs)

Pneumatic artificial muscles (PAMs) [112], also known as McKibben actuators, are one of the first generations of SPFAs. This soft actuator is composed of hollow elastomer tubes reinforced by fiber stiffness layers. Depending on their design, they will either expand or contract when pressure is applied. The invention of this artificial muscle is generally attributed to Richard H. Gaylord (1958), but it was popularized at the beginning of the 1960s by Joseph L McKibben [113]. The first SFA gripper, with four fingers, was demonstrated by Suzumori *et al* [104] in 1989 (figure 3(a)). These fingers include three chambers that give them three DOFs and can bend in any direction. This gripper can grasp a wide range of objects. There is a lot of research on soft robots that can be found using this actuation mechanism. For instance, Polygerinos *et al* [100] suggested a flexible glove for robot-assisted rehabilitation. The device utilized the McKibben mechanism not only to support precise functional grasping but also to remain light and low profile (figure 4(a)). Some approaches tried to combine multiple McKibben actuators to increase SFA functionality with more complex motions. As an example, Al Abeach *et al* [114] developed McKibben muscles for a three-fingered gripper. Both extensor and contractor McKibben designs were deployed to provide the form and efficient force for grasping ability, respectively.

PAM elastomer actuators exhibit complex nonlinear snap-through instabilities. This behavior allows the actuator to gradually store elastic energy, before releasing it suddenly to exert rapid motion or high force [115]. As shown in figure 4(b), Overvelde *et al* [116] developed this kind of nonlinear mechanism to exert high force and trigger large geometrical changes by sequential steps. Rothemund *et al* [128] designed a bistable soft valve. They calculated the required switching pressure as a function of the geometry and valve's material McKibben's muscles are also employed in the actuation of continuum robots. Tsukagoshi *et al* [117], presented an elephant trunk-type manipulator named Active Hose, consisting of a spiral tube turned around the manipulator backbone like a coil, to generate bending moment. This can be useful in rescue operations.

The other type of manipulator which benefited from PAM actuators is OctArm. It was first presented by Grissom *et al* [106] (figure 3(b)) and consists of three serial sections that are actuated separately. By applying pressure inside the chamber of each section, the arm starts simultaneously to bend and extend longitudinally for the whole-arm grasping of objects [118]. A large manipulator continuum robot with McKibben actuators consisting of six sections is reported by [119] (figure 4(c)). Applying air pressure of around four bars causes a 66% extension in section and 380° rotation in less than 0.5 s. Walker *et al* [118] in 2005 developed cephalopod robots incorporating 12 McKibben actuators. The considerable length of the robots (120 cm), acting like a manipulator, achieves more kinematic DOFs than in previous pneumatic arms and is more similar to the real biological inspiration. SPFAs can be made using highly extensible elastomer materials such as silicones. With these materials, highly deformable and adaptable soft actuators appeared. In these kinds of

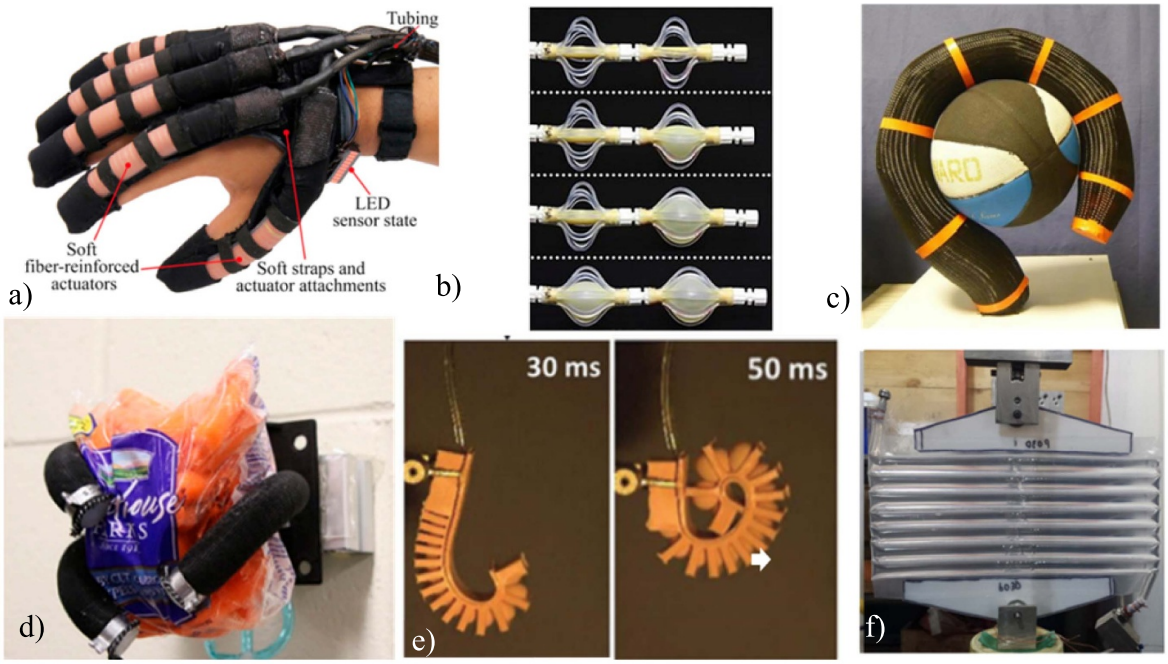

Figure 4. Some examples of SPFAs: (a) PAM mechanism used for rehabilitation gloves. Reprinted from [100] (b) Snap-through instabilities mechanism changes by sequential shape changes. Reproduced with permission from [116]. (c) Large manipulator continuum robot with McKibben's muscles. Reproduced from [119]. (d) Soft pneumatic artificial sleeved muscles. Reproduced from [125]. CC BY 4.0. (e) PneuNets actuator developed by Mosadegh *et al* [126], and (f) Peano-fluidic muscle. Reproduced from [127].

actuators, one or more embedded chambers are actuated and deformed by applying pressurized fluid, which can be operated pneumatically [94, 120,121,129], or hydraulically [122–124]. On account of their light weight and cleanness, pneumatic systems in most cases are preferred over hydraulic designs especially in gripper design (figure 4(d)) [125].

Pneumatic networks (PneuNets) are a famous pneumatic version of these actuators working as a gripper. This was first presented by Needleman [130] in 1977. He demonstrated that PneuNets, comprising a series of channels in an elastomer, can inflate like balloons for actuation. This mechanism was later developed and used as a soft gripper by Ilievski in 2011 [107] (figure 3(c)). This gripper consists of six legs for grasping soft fragile objects like an egg or even a live small animal like a mouse. In an interesting work, Mosadegh *et al* [126] developed the PneuNets architecture, achieving rapid response and more durable actuation cycles by proposing a gap layer between the walls of each chamber. Inextensible fibers are added to the FEAs to boost local stiffness and consequently the weight-object ratio in the grasping application (figure 4(e)). In [131], they employed polyaramid fibers to prevent the local weakening of the elastomer during repeated actuations. Deimel and Brock [132] developed a SPFA with a three-fingered hand and flexible palm. The fingers are made of fiber-reinforced silicone, and the palm has substantial passive compliance. The RBO Hand shows the capacity to grasp a wide variety of objects, including water bottles, eyeglasses, and sheets of fabric. Later, they presented the RBO Hand 2, composed of a five-finger and palm configuration with similar fiber-reinforced actuation technology to develop an SPFA hand [133]. It demonstrated dexterity similar to a human hand with the ability to perform most human grasping tasks.

Various types of PAMs have been developed in recent years. A famous one is a Peano-fluidic muscle presented by Veale *et al* [134]. It consists of flat layers of thermoplastic, textile reinforced plastic, or textile/silicone composite. The intervals of these layers are bonded perpendicularly in the direction of contraction. When air pressure is applied, the shapes of tubes become round with a contract ratio between 15% and 30%. The geometries of the tube affect the static and dynamic behavior of Peano-muscles [127] (figure 4(f)). The optimum channel should not exceed 20% for maximizing performance. The narrower channels increase flow restriction, subsequently, a damping force model was applied to Peano's muscle for high-accuracy controllability and further suitability in uncontrolled environments [135].

As discussed in the previous section, a similar mechanism to the Peano-muscle is the HASEL actuator. It was introduced in 2018 [64] and designed to produce linear contraction with stack (figure 3(g)). Peano-HASEL is one type of HASEL actuator, exhibits fast and precise linear motion that closely resembles muscle-mimetic activation without stack, prestretch, or rigid frames. It was developed by Kellaris *et al* [69] and made of a rectangular shell formed by flexible polymer films filled with a liquid dielectric, and planting a pair of electrodes on either side of the shell . When a charge opposes the electrodes zip together due to the electrostatic force, hence

the fluid squeezes into the volume of the shell which is not surrounded by the electrodes and creates linear contraction of the actuator. This linear actuator can lift more than 200 times its weight with a strain rate of 900% per second at 10 kV. The fast response speed, self-sensing and self-healing advantages of HASEL actuators make them a promising candidate for applications in different soft robotic mechanisms such as untethered soft robots for manipulation and continuum applications [111], tubular pump [136], and prosthetic finger driven by Peano-HASEL [137]. Rothemund *et al* [67] reviewed the latest advances and future opportunities of HASEL in the soft actuators field.

3.2. Soft vacuumed fluid actuators (SVFAs)

Vacuum mechanisms have also been widely employed in soft robots as actuators. Negative-pressure operations are safer, more compact, and more robust compared to pressurized actuators. They cannot burst when the actuator collapse. Moreover, decreasing their volume enables them to go through congested or narrow areas compared to their nominal sizes. One of the representative examples of SVFAs is the universal soft gripper developed by Brown *et al* [108] as shown in figure 3(d). Because of its simple structure, it is one of the earliest and most famous soft vacuum grippers. Unlike other soft robot actuation mechanisms, it is simply composed of a membrane filled with granular materials; the stiffness of the bag is changed by evacuating air and provides sufficient force for lifting and holding objects. It shows promising performance, especially when the shape or material properties of the object are unknown or when precise grasping is not required. This gripper was able to pick up a wide variety of objects of different sizes and shapes, such as a wooden hemisphere, spring, small LED, tube, cups, raw egg, shock absorber, etc. The device can rapidly grasp and release a wide range of objects; however, it is not appropriate for grasping flat or soft objects. The universal gripper was commercialized in [138] and has inspired several research applications, such as a prosthetic jamming terminal device [139], human collaborative robot [140], universal hand for position adjusting and assembly tasks [141], deep-sea sample-collecting device [142], flexible endoscope [143] (figure 5(a)), and soft multi-modulus manipulator for minimally invasive surgery [144] (figure 5(b)). Amend and Lipson [145] presented two simple two-fingered configurations with pockets of granular material used as end-effectors at the fingertips. This design enables each of the fingertips to work separately as independent universal grippers, or to work together like a finger and a thumb. The variable stiffness, lightweight, and energy efficiency of granular jamming make it popular for use in the soft robotics field [146]. The granule particles can be coffee, glass, plastic, or beans. The application determines the grain size; for example, powder-like granular size is generally utilized in soft robotic grippers [143, 147]. Soft manipulators, which require greater stiffness, normally employ larger grains [148]. Sayyadan *et al* [149] studied the impact of various mechanical parameters (stiffness, curvature radius, applied moment, internal stresses, and defection) on the behavior of cantilever membrane beam samples by presenting a simplified formulation under different vacuum pressure conditions. They designed various experimental tests with latex membranes filled with granular materials such as hemp, sun-dried barberries, black peppers and datura seeds.

Another important class of SVFAs was created by Yang *et al* [110] as a vacuum-actuated muscle-inspired pneumatic structure (VAMPs) (figure 3(f)). It uses the buckling of elastomeric beams to generate muscle-like motions when negative pressure is applied. Its mechanism differs from those of previous elastomeric pneumatic actuators such as PneuNets or McKibben. They can generate a linear motion similar to biological muscles. This mechanism is very similar to the performance of human muscles. Unlike other pneumatic actuation such as McKibben and PneuNets, the deformation is not obtained from area expansion and occurs inside the structure. The VAMP actuator made by Yang was able to lift 400 g. Figure 5(d) shows the performance of the VAMP. They also built a muscle-like actuator to simulate a skeleton arm moving similarly within the human body. It can contract up to 40% of its length, with loading stresses up to 65 KPa. The final displacement of the muscle is nearly five times the primary length of the VAMP. With this design, the gripper can pick up a volleyball weighing 274 g. VAMPs actuators are fast, with low cost, are easy to fabricate, lightweight, and operate safely with human interactions [150] (figure 5(c)). Verma extended Yang's works by combining a pressurized and vacuum actuator for a soft robot climbing in a tube application [154]. This climbing robot is composed of a VAMP actuator for linear motion and two ring-shaped pneumatic actuators at its extremities to hold the robot in position inside the tube. These linear actuators integrated one DOF and provided one single motion. While Jiao *et al* [151] proposed a multi-task actuator to offer many different types of motion at the same time, such as twisting, radial and linear movement (figure 5(d)). Their design included seven SVFAs to provide five crawl deformations.

Origamis are new innovative structures that have large potential use in soft robotics because of their lightweight, low-cost, easily available materials, and simple design for complex motions. They do not need hinges or joints and are actuated by applying positive or negative pressure. Therefore, according to their design and application, they can be SPFA or SVFA. Origami is the art of generating 3D structures by folding 2D sheets [155]. In [109], Martinez *et al* proposed a wide range of origami soft actuators by combining a stretchable elastomer with a non-stretchable but easily bendable sheet (figures 3(e) and 6(a)). These actuators can perform a range of complex motions that would be difficult to achieve with hard robots. Figure 6(b) shows the origami-based robotic grippers proposed by Chen *et al* [152]. It is inspired by a paper fortune teller origami design. Its reconfigurable mechanism makes the gripper be able to pick up flat-surface or non-planar objects. Li *et al* [156] suggested fluid-driven origami-inspired artificial muscles with multiaxial complex motions . Their origami actuator is fast and powerful, with a very low manufacturing cost. A soft active

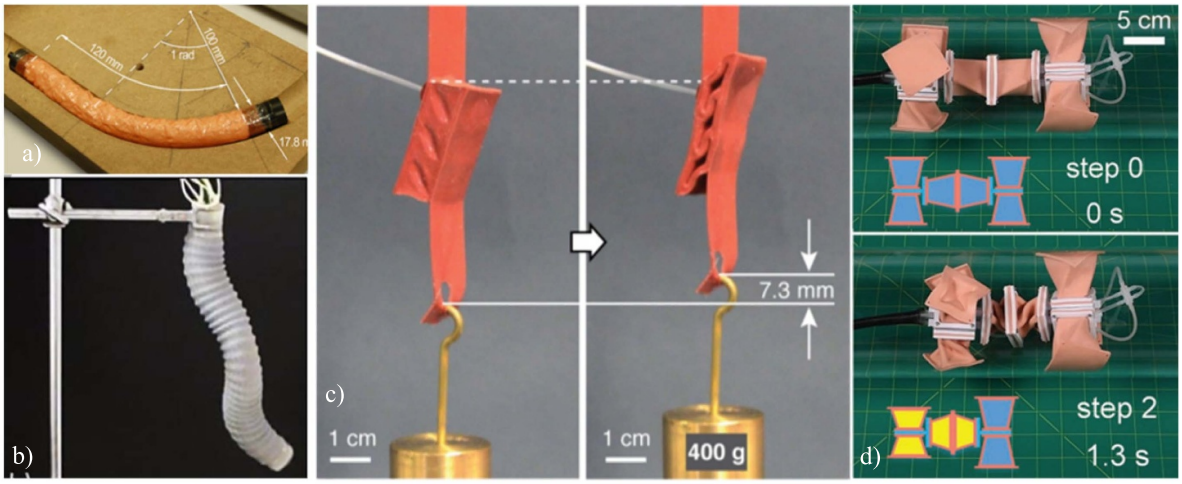

Figure 5. Some examples of SVFAs: (a) Flexible endoscope. Reproduced from [143], (b) Soft multi-modulus manipulator for minimally invasive surgery. Reproduced from [144]. (c) VAMPs actuator made by Yang *et al* [150] (d) Soft robot multi-task actuator application [151].

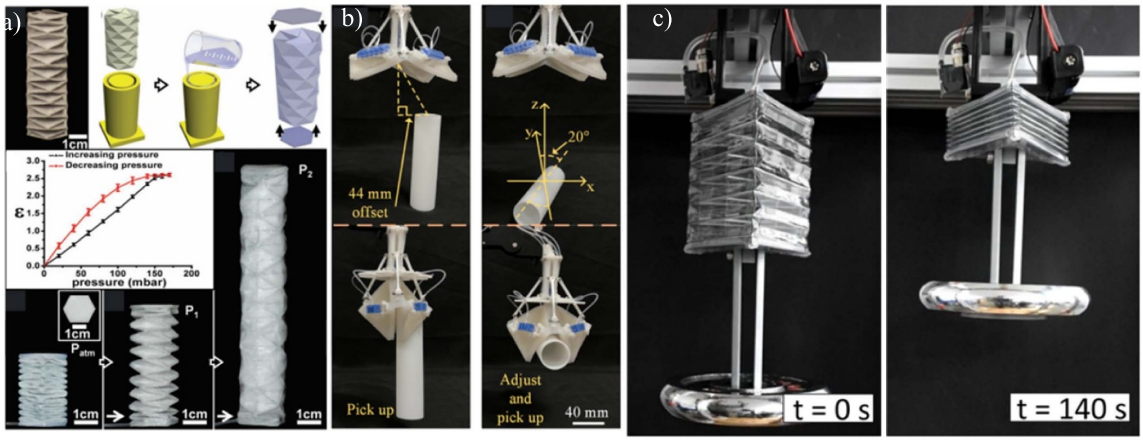

Figure 6. Origami fluidic soft actuators: (a) Combining a stretchable elastomer with a non-stretchable bendable sheet [109]. (b) Soft origami gripper. Reproduced from [152]. (c) Soft origami actuator with a payload of 1 kg. Reproduced from [153].

origami robot with a self-actuation design without the assistance of any external actuators is reported in [157]. In [153] Lee *et al* suggested a mathematical model for predicting the energy efficiency of a soft origami actuator and connected pump together. This model can be applied for the automation of low-cost off-grid operations and human-robot collaboration (figure 6(c)). Paez *et al* [158] presented a lightweight origami shell-reinforced bending module within the desired range of displacement and force requirements. Rus *et al* reviewed the design, fabrication, actuation, sensing, and control of origami robots with their applications in the different robotic areas [159].

3.3. Hybrid mechanisms

SFAs have been combined with other techniques to improve their performance, including constructability, variable stiffness, and operational range criteria. Table 2 summarizes various novel hybrid actuation approaches to address potential advances in the performance of SFAs. SMPs [160] and low melting point alloys (LMPAs) [161, 178] are deployed with SFAs to enhance shape configurability by changing and controlling the position and bending angle (figure 7(a)). Particle jamming and layer jamming can be integrated by the SFA to increase the stiffness of soft robots [162, 163, 185] (figure 7(b)). Adhesion technology such as electro-adhesive material [164] (figure 7(c)) and Gecko adhesion technique [188] (figure 7(d)) are added to SFA grippers to enhance grasping performance by increasing the lifting weight ratio and object shape diversity. Combining soft and rigid robot characteristics can build new capabilities for soft robots. For instance, Stokes *et al* proposed a hybrid soft robot consisting of a wheeled robot (hard robot part) and PneuNet SPFA (soft robot part) to manipulate and grasp an object at the same time. Pagoli *et al* [182] (figure 7(e)) introduced the innovative variable stiffness soft finger. Its soft pneumatic sliding

Table 2. The hybrid design of SFAs with other actuation mechanisms.

Hybrid design	The improvement goal	Application	Reference
SFA + SMP	Changing the bending point, shape configuration, and variable stiffness	Soft gripper	[160, 177]
SFA + LMPAs	Changing the bending point and shape configuration	Soft gripper	[161, 178]
SFA + Gecko adhesion	Higher-strength grasps at lower pressures	Soft gripper	[14]
SFA + DEA	Handling soft and delicate target objects	Soft gripper	[179]
	Minimizing the size of SFAs with 2 DoFs	Soft actuator	[180]
SFA+ Tendon	Accurate control of the bending angle by servo motor	Quadrupedal, soft gripper	[181]
	Miniaturizing the actuator	Soft gripper	[165]
SFA+ Hard robot	Changing the bending point, shape configuration, variable stiffness	Dexterous finger, soft gripper	[182, 183]
	Capable of multiple functions	Locomotion and grasping	[184]
SFA+ Electro adhesion	Gripping delicate, flat, and complex-shaped objects	Soft gripper	[164]
SFA + Layer jamming mechanism	Variable stiffness and shape control	Soft gripper	[162, 163]
SFA + Particle jamming mechanism	Variable stiffening of soft robotic actuators	Soft gripper	[185]
SPFA + SVFA	Variable stiffening of soft robotic actuators	Soft gripper	[186]
	Variable stiffening of soft robotic actuators	Minimally invasive surgery	[144]
	Linear motion	Soft climbing robot	[154]
	Increasing actuating and motion capability	Soft crawling robot	[187]

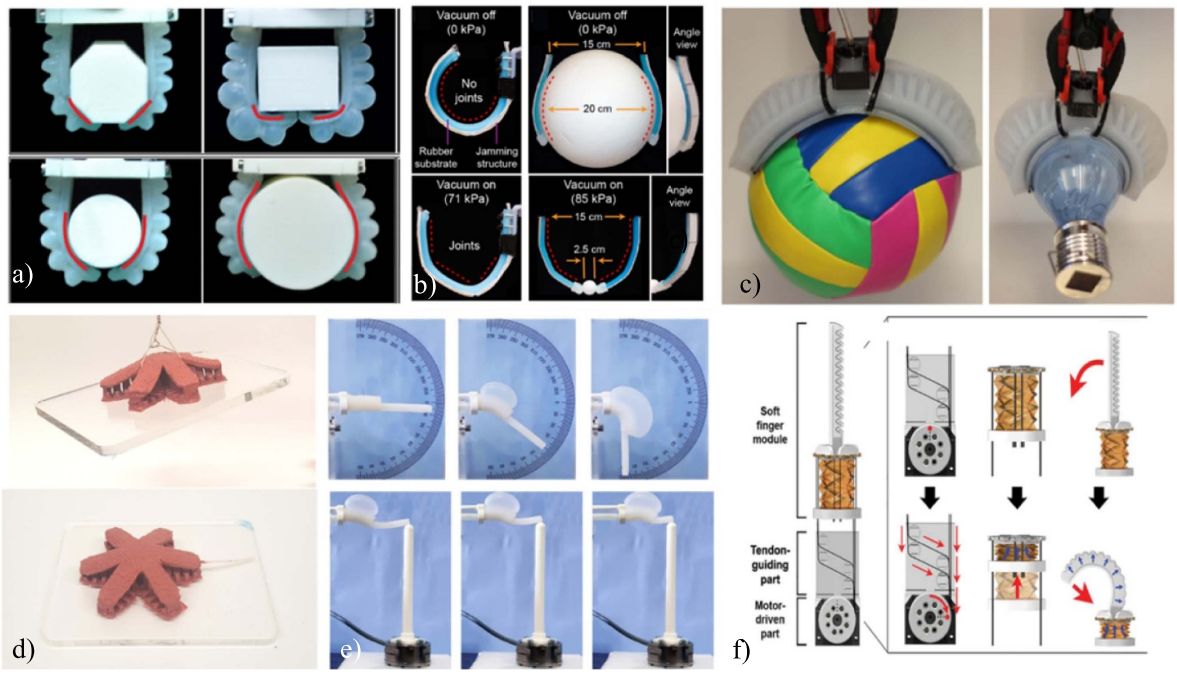

Figure 7. Hybrid design of SFAs: (a) LMPA + SPFA. Reproduced from [161]. (b) SFA + Layer jamming mechanism [162] John Wiley & Sons. © 2018. (c) Electro adhesion + SPFA. Reproduced from [164]. CC BY 4.0. (d) Gecko adhesion technique +SPFA. Reproduced from [188]. CC BY 4.0. (e) SFA+ hard: changing the bending point and variable stiffness. © [2020] IEEE. Reprinted, with permission, from [182]. (f) Tendon + SPFA Reproduced from [165]. CC BY 4.0.

joint can move and rotate along with the finger by using two electric motors. The changing position of the bending point increases the capability of the finger in terms of shape control and variable configuration. The stiffness, and consequently the applied force, at the tipping point of the finger is controlled by the pneumatic pressure inside the soft silicone link. As explained in the previous section, the climbing robot designed by Verma *et al* [154] includes two kinds of pressurized (SPFA) and vacuumed actuators (SVFA) and thus can also be classified in the hybrid design domain. Hybrid design can also be found in origami soft robots by using simultaneously positive (SPFA) and negative pressure (SVFA) to increase the actuating capability. A hybrid crawling soft robot is illustrated in [187] utilizing these characteristics for mobility. Li *et al* [181] suggested a pre-charged hybrid gripper with a combination of SPFA and tendon-driven mechanisms. The pushing/pulling cable controls the bending angle of the SPFA, the advantage of the proposed mechanism being that controlling cable movement is much easier and more accurate than pneumatic pressure. Kim *et al* [165] integrated SPFA with an origami pump which is controlled by a tendon-driven mechanism (figure 7(f)). The main advantage of the proposed gripper is that it can work without needing an external pneumatic source such as a compressor. This design helps to miniaturize soft robot actuators.

4. Material and fabrication methods

4.1. Materials of SFAs

Advances in the field of soft robotics largely depend on the knowledge of material behavior in the design of soft robotic structures and the control of these robots. Silicone rubbers are the most common material used in soft robotic systems, because of their hyper-elastic properties, lightweight, low cost, and fast and simple fabrication. Several SFA design architectures that can be found in the literature use silicone rubbers. They produce high power-to-weight ratios, requiring small input air pressures yet generating large deformations. Furthermore, they can easily be shaped into different configurations which makes them suitable for building soft actuators with a complex design. The actuation performance, such as response time, stiffness and the amount of generated force, is dependent on the type of silicone. The mechanical properties of widespread types of silicones used in soft robotic systems are listed in table 3. Several companies producing elastomer silicone can be found on the market; the most well-known brands are Smooth-On [166], Gelest [189], Dow Corning [167], and Wacker [168]. Most applications of these materials in soft robotic systems, especially in SFAs, are reviewed in this section.

EcoFlex is one of the popular silicones that are frequently used. It is commercialized by Smooth-On with several Shore hardness ratings, ranging from 00–10–00–50. The mechanical properties of three widely-used EcoFlex Shores in soft robotic applications are listed in table 3. They include hyperelasticity capability, which enables them to be streched several times their original size without rupturing. This characteristic makes them convenient in soft applications. For instance, EcoFlex 00–50 and 00–30 are very useful for developing different types of soft sensors, including prosthetic strain sensors [169], hyperelastic pressure sensors [170], flexible and wearable pressure sensors [171], healthcare biomedical wearable sensors [172], and piezoresistive sensors for human motion detection applications [173]. Furthermore, their large elongation properties make them appropriate for actuation mechanisms. Elsayed *et al* [174] studied the material properties of silicones and their effects on the bending angle of a soft pneumatic actuator. They designed and built the same geometry module with two different silicone materials, EcoFlex 00–30 and 00–50. Their experimental tests showed that the softer EcoFlex 00–30 module required a lower pressure of 0.1 bar, while the other material needed 0.32 bar to reach 90 degrees. Their approach shows that the behavior of the soft actuator is dependent on the type of silicone used. Studying and comparing different types of silicon in this review paper can thus help to select the proper material for SFA actuators. Several works on the use of EcoFlex materials in SPFAs can be mentioned. For instance, Calisti *et al* [175] proposed an octopus with six flexible limbs made from EcoFlex 00–30 with the dual capability of locomotion and grasping objects. Flexible limbs are responsible for the stability and correct balancing of the octopus in water. They also provide an effective pushing force to move the robot forward and to grasp the object by wrapping themselves around it. Tian *et al* [176] developed an SPFA human hand made of EcoFlex 00–30. It consisted of five fingers and a palm, with two joints in the thumb and three joints in the other four fingers. This soft hand can reach any point in a 3D workspace, using a variety of shapes and configurations. It also produces low resistance and carries fragile objects without damage [176].

Dragon Skin is another range of silicone commercialized by Smooth-on. Unlike the EcoFlex series, Dragon Skins have a higher Young's modulus and require more fluid pressure to actuate as SFAs. On the other hand, their greater hardness enables them to apply a larger force during actuation. Yap *et al* [190] studied and characterized the curvature radius and the force in SPFAs with different material stiffnesses. They fabricated four types of silicone rubber (EcoFlex 00–30, EcoFlex 00–50, Dragon Skin 10, and Dragon Skin 20). They defined a ratio coefficient to compare the behavior of these materials in terms of stiffness and output force by dividing the curvature radius by the original length. Their experimental results showed that for SPFAs with a 10 mm thickness, EcoFlex 00–30 achieved a minimum ratio of 0.088 at 42 kPa, while EcoFlex 00–50 reached this ratio at 52 kPa. The required pressure for Dragon Skin 10 to attain the minimum ratio of 0.092 was 180 kPa, and for Dragon Skin 20, the minimum ratio because of higher hardness was not lower than 0.199, when applying 380 kPa. On the other hand, the maximum force of the SPFA increased when the stiffness of the material increased. For example, the maximum force output for EcoFlex 00–10 and 00–50 was 2.33 at 42 kPa and 3.98 at

Table 3. Mechanical properties of the most commonly-used silicones in the Soft robotics field.

Material	Manufacturer	Shore hardness	100% Modulus (psi)	Tensile strength (psi)	Elongation at break (%)	Viscosity (cp)	Pot life (min)	Cure time (min)	Color
Silicone									
EcoFlex 00–10 [166]	Smooth-On	00–10	8	120	800	14 000	30	240	Translucent
EcoFlex 00–20 [166]	Smooth-On	00–20	8	160	845	3000	30	240	Translucent
EcoFlex 00–30 [166]	Smooth-On	00–30	10	200	900	3000	45	240	Translucent
EcoFlex 00–50 [166]	Smooth-On	00–50	12	315	980	8000	18	180	Translucent
Dragon Skin 10 [166]	Smooth-On	10 A	22	475	1000	23 000	4–20	30–300	Translucent
Dragon Skin 20 [166]	Smooth-On	20 A	49	550	620	20 000	25	240	Translucent
Dragon Skin 30 [166]	Smooth-On	30 A	86	500	364	20 000	45	960	Translucent
Sylgard 184 [167]	Dow Corning	43 A	—	980	100	5100	90	2880	Translucent
Elastosil M4601 [168]	Wacker	28 A	75 [150]	943	700	10 000	90	720	Reddish-brown
ExSil 100 [189]	Gelest	15 A	29	870–1015	4000–6000	12 000–14 000	1440	240 at 80 °C	Translucent
Sil 940 [166]	Smooth-On	40 A	200	600	300	35 000	30	1440	Pink
Sil 950 [166]	Smooth-On	50 A	272	725	320	35 000	45	1080	Blue
Sil 960 [166]	Smooth-On	60 A	280	650	270	30 000	45	960	Green
Mold Star 30 [166]	Smooth-On	30 A	96	420	339	12 500	45	300	Blue
RTV615 [191]	Momentive	44 A	—	920	120	4000	240	6–7 d	Translucent
RTV-KE-1603 [192]	ShinTsu	28 A	—	508	450	—	90	1440	Translucent
3D Printer Materials									
FilaFlex [193]	Recreus	82 A	—	—	700 (DIN 53 504)	—	—	—	—
NinjaFlex [194]	NinjaTek	85 A	—	580(ASTM D638)	660(ASTM D638)	—	—	—	—
Agilus30 [195]	Stratasys	30–35 A	—	348–450 (ASTM D 412)	220–270 (ASTM D 412)	—	—	—	—
		30–40 A	—	305–377	185–230	—	—	—	—

52 kPa respectively. For Dragon Skin 10 and Dragon Skin 20, the output force ratio was higher, reaching 8.82 at 180 kPa and 9.96 at 380 kPa, respectively.

Another popular silicone rubber in soft robot applications is Sylgard 184, due to its characteristics, including optical transparency, low viscosity, average tear resistance, and the ability to be sealed by plasma-activated surface bonding [196]. It is commercialized by Dow Corning [197]. The viscosity and Young's modulus of this silicone are 3500 cp and 3.9 MPa respectively. The high modulus of Sylgard 184 makes it a stiff and inappropriate choice for SFA applications, since it requires a higher pressure than EcoFlex to function as an actuator. However, it can be useful, especially in soft grippers if integrated with other actuation methods such as DEA [198] or Gecko adhesion [199]. It is also found in a wide range of sensor products, e.g. capacitive strain sensor [200], pressure sensor [201], and tactile sensor [202]. White *et al* [203] fabricated Sylgard 184 silicone layers with gallium–indium alloy as a resistant sensor to measure the geometry changes due to deformations. They were deployed to build a sensor for soft robots. This sensor was able to measure uniaxial strain and curvature, and could be applicable in soft skin sensors. In a similar approach, Markvicka *et al* [204] studied the mechanical behavior of an elastomer composite with four different blends of Sylgard 184 and Sylgard 527 containing liquid metal droplets. It ruptured when mechanical damage occurred and could be a suitable sensor for damage detection in soft robots with self-healing properties.

In recent years, self-healing materials have been developed to recover their structure entirely from mechanical damage, without using external stimuli [205]. This autonomous capability increases the commerciality of SFAs, especially in unstructured environments. On the other hand, self-healing polymers are usually more expensive and require more synthetic steps and chemical modification processes [206]. Diels–Alder networks are popular thermo-reversible polymers deployed by Terryn *et al* [207] to heal SFAs ripped, perforated, or scratched by sharp objects. Later they have shown the safe healing ability of SFA's applications in safe human-robot interactions such as social robots, household robots, and hand rehabilitation devices. Shepherd *et al* [131] developed a soft fluid actuator integrated with polyaramid fibers (Kevlar) reinforcement. After actuating with positive pressure, this SFA could seal itself after being punctured with a 14-gauge needle. Even after removing the needle, the pressure was retained inside the chamber [208]. Bilodeau *et al* [209] reviewed recent advanced and future self-healing applications and damage-resilient materials in soft robotic systems.

Elastosil M4601 is commercialized by the Wacker Chemical company and can be found in some of the soft robotics literature. As shown in table 3, its Shore hardness and Young's modulus are very similar to Dragon Skin 30, but unlike EcoFlex and the Dragon Skin series, it has low optical transparency, which limits its applications as a soft opto-electronic sensor. Nevertheless, its higher stiffness makes it a good option for soft actuators, especially in soft gripper applications. Galloway *et al* [210] developed an underwater two-opposing-pairs soft robotic gripper made using M4601 silicone to manipulate fragile and delicate samples on deep reefs. By applying a 310 kPa pressure, the gripper can produce a 52.9 N lift force. Mosadegh *et al* [126] replaced the soft EcoFlex with a stiffer Elastosil M4601 and the actuation pressure increased eight times for the same bending angle. Robertson *et al* [211] suggested four parallel SPFAs made of M4601 to produce a higher force, around 112 N. This is 23% more than the volumetrically equivalent single SPFA. These experiments demonstrated the interest of utilizing a multiple SPFA for high-performance soft robotic applications rather than existing uniform and non-optimal SPFA designs. At room temperature, EcoFlex 00–30 (with a Shore hardness 00–30) has the shortest pot life of 45 min, while this value for Elastosil M4601 with a Shore hardness of 28 A and Sylgard 184 with Shore hardness of 43 A are 90 min. Wienzek *et al* [212] studied the increase in long-term storage of mixed silicone liquid at low temperature for the strain-limiting top layer of a soft gripper. They tested three types of silicone samples (Elastosil M4601, EcoFlex 00–30, and Sylgard 184). They mixed and maintained the samples at −25 °C for 12 weeks. Viscosity was measured weekly to determine the curing characteristics. The results show that EcoFlex 00–30 solidified after 14 d, while the mixed sample solutions of Elastosil M4601 and Sylgard 184 were still liquid and usable for casting processes after period of 8.7 and 12 weeks, respectively. This study helps to separate the mixing and molding process and increase the fabrication options for silicones.

As listed in table 3 for the production of SFAs, some approaches utilize other types of silicone, such as translucent RTV615 [213] with Shore hardness 44 A and commercialized by Momentive, translucent KE-1603 with Shore hardness 28 A [214, 215], blue color Mold Star 30 A [216], and ExSil 100 with Shore hardness 15 A. ExSil 100 was first introduced by Goff *et al* [217] and later commercialized by Gelest. Although it has high elongation up to 5000%, its Young's modulus is 0.02 MPa, which makes it too soft to use as an actuator or gripper. It is normally used in diaphragms, microfluidics, vibration damping, high-performance seals, optics and electrical interconnectors [189].

As explained before, the stiffness and generated force in SFAs are dependent on the type of silicon. Considering this, some approaches combine different types of silicone materials to attain the desired stiffness. Shepherd *et al* [94] developed a multigate walking robot with different silicone layers. Due to its high extensibility under low stresses, EcoFlex 00–30 was used as the actuating layer, and Sylgard 184 was selected as a strain-limiting layer. This combination not only enables the soft robot to operate at low pressures (7 psi), but also provides the desired stiffness. In their next approach [129], these authors replaced the actuation layer of EcoFlex 00–30 by M4601 to increase to larger loads such as the weight of the robot body and components for untethered operation; inevitably, material of this hardness requires higher pressure actuation (22 psi). Hassan *et al* [218] proposed a tendon-actuated soft three-finger gripper made by using three different types of soft materials: Dragon Skin 30, Smooth-Sil 950, and a

third type manufactured by combining Smooth-Sil 950 with EcoFlex 00–30. The intrinsic properties of Dragon Skin 30 make it sticky compared to Sil 950. Thus, the first soft gripper made using Dragon Skin 30 shows a better performance with respect to slipping than the second one. To overcome this limitation in the second gripper, they suggested attaching silicone strips made of Smooth-Sil 950 with EcoFlex 00–30 on the surface of the third gripper to guarantee stable grasping for lateral bending. Subramaniam *et al* [216] developed a multi-material SVFA gripper with an active palm for grasping applications. They used different types of silicones such as Mold Star30, Smooth Sil 940, Smooth Sil 960, and EcoFlex 00–30 to achieve the desired stiffness, Mold Star30 was selected for the skin layer because of its high deformation at low pressures.

All the silicone materials presented in the previous paragraphs use molding techniques, while in recent years additive manufacturing (AM) techniques such as 3D printing have also been employed to directly fabricate SFAs. The most successful fused deposition modeling (FDM) material for soft robotics is NinjaFlex (Shore hardness of 85 A) made of thermoplastic polyurethanes (TPU), which can withstand strains above 700% with a Young's modulus of around 10 MPa. The SPFAs that are printed using this method can produce a blocking force of up to 75 N [102]. FilaFlex [219] and Agilus30 [220, 221] are the other two types of TPUs employed to print SFAs. The mechanical properties of these materials and their suppliers are listed in table 3. The manufacturing methods of SFAs, and especially 3D printing technology, will be discussed in a dedicated section.

4.2. Manufacturing and fabrication of SFAs

The classical molding method can be used to fabricate different designs of the SFA actuator [222]. Thanks to the latest developments in 3D printing technology, the design of mold parts has improved significantly, which enables the designer to make complex soft components with more accuracy. Normally, catalyzed silicone rubber consists of two parts that should be mixed homogeneously with the specified ratio according to the manufacturer's instructions. In most cases vacuum degassing for 4–5 min is suggested to avoid air entrapment. An alternative and more effective way is putting the mixed silicone into a centrifuge machine. Cure time is variable and differs from 30 min to 1 d at room temperature, depending on the silicone viscosity. This time can be reduced to less than an hour by putting the mixed liquid in an oven at a temperature of around 70 °C [223]. Molding complex structures, especially with undercuts and internal architectures, is very difficult [224]. To overcome this problem, AM methods have also been proposed [225].

SFAs can be printed directly using 3D printers. The FDM method is one of the most widely-used techniques for material fabrication using 3D printers, at low cost and eliminating any supporting molding material, easing changes in the material, and also reducing the fabrication time. The working principle is based on a heating filament and horizontally depositing molten materials via extrusion nozzle onto a surface, layer by layer. NinjaFlex is the most common material used in the 3D printing of SFAs, due to its high strain and force-producing ability when used as an actuator [102, 226]. Peele *et al* [227] used the stereolithography (SL) technique to produce a SPFA layer by layer from an elastomeric precursor material. The proposed DMP-SL printing process is a promising way to fabricate a monolithic actuator in one single process. In the SL approach, the solidification of liquid resin is controlled by photo-polymerization by a laser beam or a digital light projector. In SL, unlike FDM, one resin can be printed at one time, and this is the major potential challenge of using this technique. For more information about 3D printing methods, the reader is referred to the review articles [228–230].

5. Modeling

Based on previous research, SFA models can be classified into three main groups: analytical methods, numerical methods, and model-free methods. In this section, we present the latest advances and potential challenges in each category.

5.1. Analytical methods

The earliest analytical model for SPFAs is Euler-Bernoulli's beam theory. In this theory, SPFAs are assumed to be cantilever beams with a fixed support on one side and a moment on the other side. The model is useful when SFAs have simple (particularly symmetric) structures. Several works can be found in the literature using this theory, such as bi-bellow actuators with three chambers developed by Shapiro [231], pneumatic bending joints with anisotropic rigidity [232], and soft biomimetic robotic fish [233]. This theory is not applicable for hyperelastic material with large bending deformations such as silicone, where cross-sectional planes do not remain perpendicular to the bending moment axis. Some approaches have been tried to improve the result of this method. In most of the previous works, Young's modulus is assumed to be constant, while experimental results show that the stress–strain behavior of these materials is more complex, and the relation between cross-section and curvature radius cannot be found easily [234]. The analytical method approach is more successful in continuum robot modeling, especially when the material is not hyperelastic. The backbone curve approach [235] was the first kinematic model for continuum robots. Later, the constant curvature model (CCM) [54] was suggested for the kinematics of multi-section soft robots. Trivedi *et al* [236] deployed the work-energy principle to develop a geometric model for SPFA manipulators, and showed that their model is more accurate than the CCM. Polygerinos *et al* [237] used analytical methods to model SPFA with fiber-reinforced bending pneumatic actuators. Wang *et al* [238] presented a simplified model of a soft pneumatic gripper with simple line links connected by a set of viscoelastic joints. In conclusion, SPA analytical models come with a lot of approximations and

simplification in terms of shape and material properties, which make them inaccurate and require a robust controller to compensate for this lack of accuracy.

5.2. Numerical methods

5.2.1. Off-line FEM simulation. Due to the highly nonlinear responses of silicone rubbers, modeling and analyzing SPFAs is quite challenging. The finite element method (FEM) has widely been considered to predict the behavior of SPFAs. Material properties, configuration cross-sections, compressibility effects of the pneumatic cavity, and actuation boundary conditions can be defined in the FEM software, and contribute to increasing simulation accuracy. Because of the powerful FEM tools available to model hyperelastic materials, various FEM solutions have been introduced in the literature. Optimal design is the other advantage of using FEM simulation to meet specific performance criteria such as reducing the geometry dimensions [239], improving actuating speed [126], or enhancing the performance of soft actuators by maximizing the bending angle [221, 240]. Particularly in a commercial application, it is necessary to use FEM optimization once and then produce the SPFAs and prerequisites such as molding devices to reduce the production costs and time. In table 4, we summarize the different FEM solvers and the material properties which are used to predict the hyperelastic characteristics of silicone. Silicone rubber is modeled as an isotropic, incompressible and hyperplastic material. The mechanical behavior of hyperelastic materials is characterized by the strain energy function U, which is then given by [241]:

$$U = \sum_{i+j=1}^{N} C_{ij}(\bar{I}_1 - 3)^i(\bar{I}_2 - 3)^j + \sum_{i=1}^{N} \frac{1}{k_i}(J_{el} - 1)^{2i} \quad (1)$$

where U is the strain energy potential per unit volume, $N$is the polynomial order, $\bar{I}_1$and $\bar{I}_2$ are the deviatoric strain invariants, $C_{ij}$is a material-specific parameter, J_{el} is the elastic volume ratio and k_i expresses compressibility. Considering the silicone as an incompressible material, the term k_i is omitted, which simplifies the general polynomial form of the strain energy potential. (1) can be fitted by different hyperelastic models, i.e. Mooney–Rivlin, Yeoh, Ogden, or Neo-Hookean models.

- Mooney–Rivlin material model

This model was one of the first hyperelastic models used to predict the nonlinear behavior of isotropic hyperelastic materials [242]. The strain-energy function for this material model is:

$$U = \sum_{i=1}^{N=2} C_i(\bar{I}_i - 3)^i. \quad (2)$$

- Ogden material model

Based on the theory of elasticity, the Ogden model was developed first time by Ogden [243] and has the general form:

$$U = \sum_{i=1}^{N} \frac{2\mu_i}{\alpha_i^2}(\lambda_1^{\alpha_i} + \lambda_2^{\alpha_i} + \lambda_3^{\alpha_i} - 3). \quad (3)$$

where μ_i and α_i are material constants and λ, are principal stretches.

- Yeoh material model

This model was first presented in 1990 for incompressible materials [244]:

$$U = \sum_{i=1}^{3} C_i(\bar{I}_1 - 3)^i. \quad (4)$$

As shown in this equation, the strain-energy function in this model relies only on the first strain invariant ($\bar{I}_1$).

- Neo–Hookean material model

It was presented by Holzapfel [267]. For the Neo–Hookean material model, the function of the strain energy is related to a linear equation for the principal strains

$$U = C_1(\bar{I}_1 - 3). \quad (5)$$

Table 4 summarizes the coefficients of these equations based on previous approaches in the literature. These constant parameters are calculated by stress–strain experiments. The uniaxial test is more widespread and typical than biaxial and planning tests. Selecting and designing the most appropriate test for the specimen of silicone increases the accuracy of the model parameters. Several approaches were studied to predict the nonlinear elastic behavior of silicone rubber under different loading conditions in order to understand the mechanics by finding the best least square curve fitting the potential strain energy function. Marechal *et al* [245] provided a database of the best constitutive models and the values of the coefficients according to uniaxial tensile tests recommended in the ASTM D412 for elastomers. Each silicone specimen was cured at room temperature with the nominal mixing ratio recommended by the manufacturers. We deployed this database to compare different suggested constitutive models in the previous approaches listed in table 4. The results for different silicone materials are shown in figure 8. Abaqus is used as the framework to reproduce the curve fitting of the suggested constitutive model in each reference. Although the treatment conditions, such as degassing, natural aging or the addition of pigment may affect the mechanical properties of the hyperelastic materials in this simulation, we assumed that these models were extracted in general conditions, such as the mixing ratio recommended by the manufacturer and curing at room temperature, without considering differences in the testing process and measurement equipment. Furthermore, most of the reviewed articles do not mention which type of test data, true

Table 4. Material modeling for various types of silicone for soft fluidic.

Material	Treatment	Software	Model	Coefficient (MPa)	References
EcoFlex 00–10	—	ABAQUS	Ogden ($N = 1$)	$\mu_1 = 12.605 \times 10^{-3}, \alpha_1 = 4.32$	Sparks *et al* [249]
EcoFlex 00–30	Curing at 120 °C for 60 min after vacuum degassing (EcoFlex) Strain rate: 300 mm min^{-1}	ABAQUS	Yeoh	$C_{10} = 5.072 \times 10^{-3}, C_{20} = -3.31 \times 10^{-4}$, $C_{30} = -1.5 \times 10^{-5}$	Elsayed *et al* [174]
	ASTM D638, strain rate: 500 mm min^{-1}	ABAQUS	Yeoh	$C_{10} = 0.012662$	Polygerinos *et al* [237]
	ASTM D412, curing at room temperature	ABAQUS	Ogden ($N = 3$)	$\mu_1 = 0.024361, \alpha_1 = 1.7138$, $\mu_2 = 6.6703 \times 10^{-5}, \alpha_2 = 7.0679$, $\mu_3 = 4.5381 \times 10^{-4}, \alpha_3 = -3.3659$	Moseley *et al* [240]
	—	ABAQUS	Ogden ($N = 3$)	$\mu_1 = 1.887 \times 10^{-3}, \alpha_1 = -3.848$, $\mu_2 = 2.225 \times 10^{-2}, \alpha_2 = 0.6632$, $\mu_3 = 3.574 \times 10^{-3}, \alpha_3 = 4.225, D_1 = 2.9259$	Agarwal *et al* [250]
	Curing at 60 °C for 15 min after vacuum degassing	ABAQUS	Arruda-Boyce	$\mu = 0.03, \lambda = 3.9$	Martinez *et al* [251]
	Curing at 55 °C for 20 min after vacuum degassing	ABAQUS	Yeoh	$C_{10} = 7.61 \times 10^{-3}, C_{20} = 2.42 \times 10^{-4}$, $C_{30} = -6.2 \times 10^{-7}$	Sareh *et al* [246]
	ISO 527–3	ABAQUS	Ogden ($N = 3$)	$\mu_1 = 2.2 \times 10^{-2}, \alpha_1 = 1.3, \mu_2 = 4 \times 10^{-4}$, $\alpha_2 = 5, \mu_3 = -2 \times 10^{-3}, \alpha_3 = -2$	Steck *et al* [252]
		ABAQUS	Yeoh	$C_{10} = 1.7 \times 10^{-2}, C_{20} = -2 \times 10^{-4}$, $C_{30} = 2.3 \times 10^{-5}$	
	—	ABAQUS	Neo-Hookean	$C_{10} = 0.01$	Subramaniam *et al* [216]
	ASTM D412, the strain rate of 450 mm min^{-1}, curing at room temperature with vacuum degassing	Developed Python code	Ogden ($N = 3$)	$\mu_1 = -0.322, \alpha_1 = 3.31, \mu_2 = 0.19$, $\alpha_2 = 3.115, \mu_3 = 0.145, \alpha_3 = 3.468$	Marechal *et al* [245]

(Continued.)

Table 4. (Continued.)

Material	Treatment	Software	Model	Coefficient (MPa)	References
EcoFlex 00–50	Curing at 120 °C for 60 min after vacuum degassing (EcoFlex)	ABAQUS	Ogden ($N = 3$)	$\mu_1 = 107.9 \times 10^{-3}, \alpha_1 = 1.55,$ $\mu_2 = 21.47 \times 10^{-6}, \alpha_2 = 7.86,$ $\mu_3 = -87.1 \times 10^{-3}, \alpha_3 = -1.91$	Elsayed *et al* [174]
	—	ABAQUS	Yeoh	$C_{10} = 1.9 \times 10^{-2}, C_{20} = 9 \times 10^{-4},$ $C_{30} = -4.75 \times 10^{-6}$	Runge *et al* [253]
	—	ANSYS	Hookean	—	Nasab *et al* [254]
	Strain rate: 0.2 mm s^{-1}	—	Mooney-Rivlin	$C_1 = 10.401 \times 10^{-3}, C_2 = 21.362 \times 10^{-3}$	Pineda *et al* [255], Lee *et al* [256]
	ASTM D412, the strain rate of 450 mm min^{-1}, curing at room temperature with vacuum degassing	Developed Python code	Ogden ($N = 3$)	$\mu_1 = 1.97, \alpha_1 = 2.911, \mu_2 = -3.671,$ $\alpha_2 = 3.008, \mu_3 = 1.740, \alpha_3 = 3.096$	Marechal *et al* [245]
Dragonskin 10	—	ABAQUS	Yeoh	$C_{10} = 36 \times 10^{-3}, C_{20} = 2.58 \times 10^{-5},$ $C_{30} = -5.6 \times 10^{-7}$	Sareh *et al* [246]
	ISO 37, strain rate: 450 mm min^{-1}, curing at room temperature with vacuum degassing	ABAQUS	Ogden ($N = 3$)	$\mu_1 = -1.8261, \alpha_1 = 1.613, \mu_2 = 1.12,$ $\alpha_2 = 2.0184, \mu_3 = 0.7951, \alpha_3 = 0.9386$	Byrne *et al* [257]
	—	ANSYS	Mooney–Rivlin	$C_{10} = 0.04, C_{01} = -0.033, C_{11} = 1.2 \times 10^{-3}$	Basturen *et al* [258]
	ASTM D412, Strain rate of 500 mm/min	—	Yeoh	$C_{10} = 7.61 \times 10^{-3}, C_{20} = 2.42 \times 10^{-4},$ $C_{30} = -6.2 \times 10^{-7}$	Low *et al* [247]
	ASTM D412, the strain rate of 450 mm min^{-1}, curing at room temperature with vacuum degassing	Developed Python code	Ogden ($N = 3$)	$\mu_1 = 1.971 \times 10^{-19}, \alpha_1 = 18.341,$ $\mu_2 = 1.03, \alpha_2 = 2.729, \mu_3 = -1.059, \alpha_3 = 2.649$	Marechal *et al* [245]
Dragon Skin 30	Strain rate: 300 mm/min	ABAQUS	Yeoh	$C_{10} = 1.19 \times 10^{-3}, C_{20} = 2.3 \times 10^{-2}$	Elsayed *et al* [174]
	—	ANSYS	Ogden ($N = 1$)	$\mu_1 = 75.449 \times 10^{-3}, \alpha_1 = 5.836$	Heung *et al* [259]
	—	ANSYS	Ogden ($N = 1$)	$\mu_1 = 0.1581, \alpha_1 = 2.7172$	Al-Rubaiai *et al* [248]
	ASTM D412, the strain rate of 450 mm min^{-1}, curing at room temperature with vacuum degassing	Developed Python code	Mooney–Rivlin	$C_{10} = 0.247, C_{01} = -0.33, C_{20} = 2.09 \times 10^{-4}$	Marechal *et al* [245]

(Continued.)

Table 4. (Continued.)

Material	Treatment	Software	Model	Coefficient (MPa)	References
Elastosil M4601	ASTM D638, strain rate: 500 mm/min	ABAQUS	Yeoh	$C_{10} = 0.11, C_{20} = 0.02$	Polygerinos *et al* [237], Zhang *et al* [260]
	—	ABAQUS	Hookean	$E = 0.54$ MPa	Yang *et al* [261]
	ASTM D638	ABAQUS	Yeoh	$C_{10} = 0.125, C_{20} = 0.0075$	Wang *et al* [262]
	Curing at 70 °C for 20 min	ANSYS	Hookean	$E = 0.387$	Hu *et al* [263]
	ASTM D638	—	Mooney-Rivlin	$C_1 = 10.401 \times 10^{-9}, C_2 = 21.362 \times 10^{-9}$	Ogura *et al* [215]
Silica gel	—	ABAQUS	Yeoh	$C_{10} = 0.036, C_{20} = 0.007$	Zhang *et al* [264]
Agilus30		ABAQUS	Mooney-Rivlin	$C_{10} = -0.4889, C_{01} = 0.7147,$ $C_{11} = -0.2704, C_{20} = 0.07929,$ $C_{02} = 0.4709, D_1 = 0.4574, D_2 = 0$	Pasquier *et al* [220], Chen *et al* [221]
SmoothSil 960	Curing at room temperature for 24 h	ABAQUS	Neo-Hookean	$C_{10} = 0.17$	Subramaniam *et al* [216]
SmoothSil 940	—	ABAQUS	Neo-Hookean	$C_{10} = 0.12$	Subramaniam *et al* [216]
MoldStar 30	—	ABAQUS	Neo-Hookean	$C_{10} = 0.055$	Subramaniam *et al* [216]
Elastomeric Precursor	—	ANSYS	Hookean	—	Peele *et al* [227]
RTV-KE1603	Curing at room temperature after vacuum degassing	MSC Marc	Mooney–Rivlin	$C_{10} = 8.635 \times 10^{-2}, C_{01} = 6.213 \times 10^{-2},$ $C_{11} = -1.2896 \times 10^{-2}, C_{20} = 3.425 \times 10^{-3},$ $C_{02} = -6.577 \times 10^{-1}$	Wakimoto *et al* [214], Ogura *et al* [215]
NinjaFlex	Printing temperature: 245 °C	ABAQUS	Ogden ($N = 3$)	$\mu_1 = -30.921, \alpha_1 = 0.508, \mu_2 = 10.342,$ $\alpha_2 = 1.375, \mu_3 = 26.791, \alpha_3 = -0.482$	Yap *et al* [102]
	ISO 37, strain rate: 100 mm s^{-1}, printing Temperature 240 °C	ANSYS	Mooney–Rivlin	$C_{10} = -2.33 \times 10^{-1}, C_{01} = 2.562,$ $C_{11} = -0.561, C_{20} = 0.9$	Tawk *et al* [265, 266]
FilaFlex	Printing temperature: 235 °C	ANSYS	Mooney–Rivlin	$C_{10} = 1.594, C_{01} = 0.44, C_{11} = -4.4 \times 10^{-3}$	Hu *et al* [219]

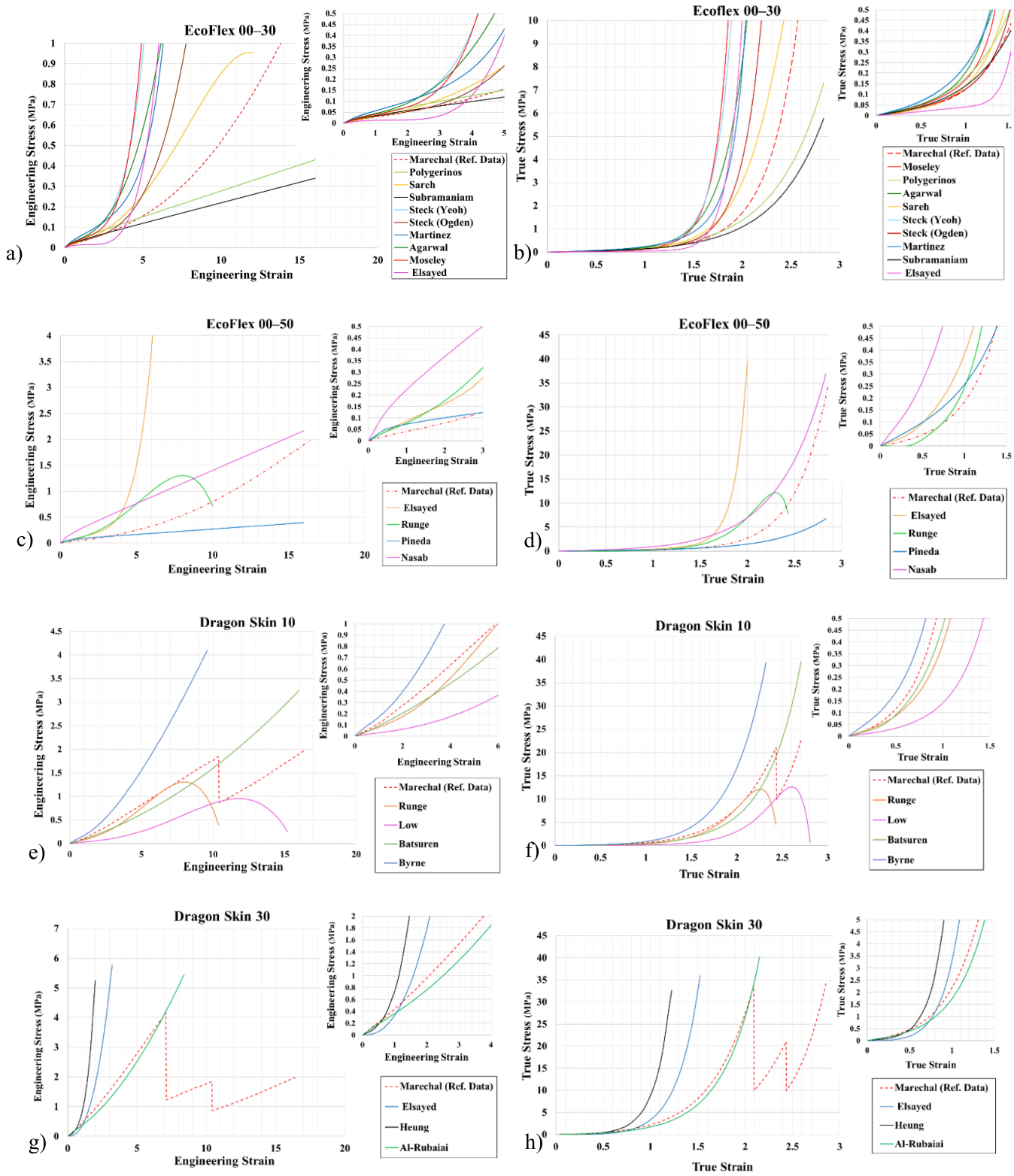

Figure 8. Comparison of the responses of proposed constitutive models for silicone materials in different references with uniaxial experimental standard test data from Marechal *et al* [245]: (a) Engineering stress–strain comparison of EcoFlex 00–30. (b) True stress–strain comparison of EcoFlex 00–30. (c) Engineering stress–strain comparison of EcoFlex 00–50. (d) True stress–strain comparison of EcoFlex 00–50. (e) Engineering stress–strain comparison of Dragon Skin 10. (f) True stress–strain comparison of Dragon Skin 10. (g) Engineering stress–strain comparison of Dragon Skin 30. (h) True stress–strain comparison of Dragon Skin 3.

or engineering strain-stress, were used to predict the material models. Note that engineering stress, also known as nominal stress, is calculated by dividing the applied force by the primary cross-section area of the material, while in true stress this area is changed and calculated with respect to time. We extracted the true and engineering strain-stress data from the proposed constitutive models in these articles using ABAQUS software. These figures help to compare the models by assuming that the experimental protocol is the same and based on ASTM D412. We take Marechal's test data as the reference and compare it with the other models for each type of silicone, by true and engineering stress versus strain results, as presented in figure 8. This figure shows the experimental data compared with the best-fitting FE models results for the various silicone rubbers. As shown in (figures 8(a) and (b)), for EcoFlex 00–30 in a small stress–strain range, most of the models are fitted with acceptable divergence. The Yeoh model suggested by Sareh *et al* [246] fits the experimental data with few differences. In the EcoFlex 00–50 graphs (figures 8(c) and (d)) the variation between the proposed models and raw experimental data is obvious even for small stress–strain values. The Yeoh model by Low *et al* [247] (figures 8(e) and (f)) and the first-order Ogden model by Al-Rubaiai *et al* [248] (figures 8(g) and (h)) predict the behavior of Dragon skin 10 and 00–30 respectively with minimum divergence, even in large stress values.

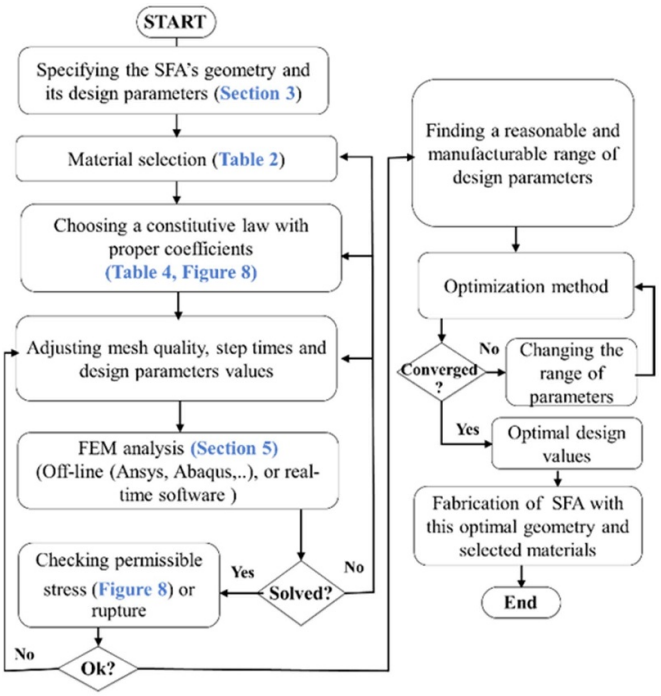

Figure 9. A flowchart of the fabrication procedure of SFA step by step from choosing material to build a prototype.

5.2.2. Real-time FEM simulation. Although FEM software applications such as Abaqus and Ansys can generate precise calculations of SPFA, their slow simulation speed restricts their usage in real-time problems. To speed up the simulation, real-time software has been developed in recent years. One of the real-time simulation engines that provide several iterative algorithms and mechanical models for users is SOFA. It was first released in 2007 [268]. Due to its open-source availability, it has steadily evolved and different libraries such as a soft robot plugin have been added by users. SOFA uses general layers such as an internal model with independent DOFs, mass and material constitutive laws, a collision model, and a visual framework for modeling an object [269]. Dynamic control of SPFA is another advantage of using SOFA for simulation/control co-design procedures [270, 271]. SOFA can interact with other software to co-design the controller; in this case, SOFA is a real-time FEM simulator and Matlab/Scilab are the control designer simulation engine [272]. However, real-time constraints make the method possible only for relatively coarse meshes and simple material constitutive laws. Furthermore, anisotropic material models are not available in SOFA and must be integrated with additional simulator codebases [193].

Vega-FEM is a free and open-source middleware C/C++ library for simulating 3D deformable objects based on physics rules. In Vega, various linear and nonlinear material models can be implemented, including linear and co-rotational FEM elasticity, Saint-Venant Kirchhoff FEM model, invertible FEM models, and mass-spring systems [273]. It can efficiently predict the behavior of deformable materials such as silicone, and provides the base infrastructure to implement additional force models [274]. The potential challenge in Vega is it cannot correctly implement collision detection or contact points, so its application in contact approaches is limited [275]. Like SOFA, Voxelyze is another multi-material Open Dynamics Engine for general static and dynamic analysis suggested by Hiller *et al* [276]. It works based on lattice of voxels of discrete points connected by spring-like beam elements including translational and rotational stiffness to simulate very large deformations and heterogeneous properties under an applied force. Although some applications of Voxelyze have been reported on soft robots [277, 278], it has some limitations which hinder its wide expansion. For instance, a precise approximation of some geometrical shapes requires an increase in the number of voxels, which increases computation time. Moreover, beam theory in Voxelyze is used for the mechanical modeling of the object, which is different from the realistic deformation behavior of continuous material.

5.3. Model-free methods

The obstacles we have discussed to developing analytical and numerical models have led to research attempts being made to control soft robots using nonparametric methods based on learning or vision. These aim to be a more efficient alternative. Lee *et al* [279] proposed a nonparametric local learning technique to learn the inverse kinematics and control of SFAs. The model is able to predict the end-effector position of the robot accurately in the presence of an external dynamic disturbance. They utilized FEM to generate a sample of kinematic data to pre-train the initial control. A neural network

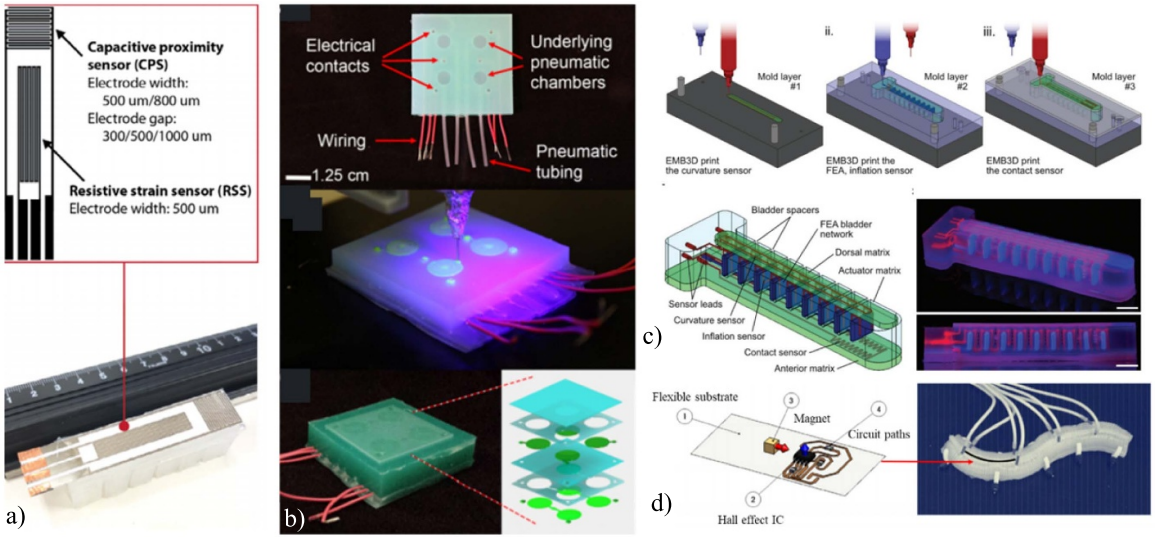

Figure 10. Soft fluidic actuators with integrated sensors: (a) Combining resistive and capacitive sensors. Reproduced from [293]. CC BY 4.0. (b) Using a 3D printer to integrate hydrogel electrodes into silicone as a tactile sensor. Reprinted from [296], (c) 3D printed a soft actuator ionically conductive gels [299] (d) Embedded magnetic curvature sensor in SFA. Reprinted from [303].

was applied in [280] to control a 1-DOF SPFA, with a vision-based motion capture system acquiring unknown soft actuator parameters. A feedforward neural network to learn the 3D nonlinear inverse kinematic model of a soft octopus-arm was implemented and tested in [281]. The potential challenges of this method are the accuracy of the training-based kinematic computation, dependent on properly selected datasets. Several works can be found in the literature concerning the visual servoing of soft actuators. Li *et al* [282] proposed an adaptive Kalman filter for continuum robot path tracking. They used pressures and tip position as input data. Then they estimated the robot's Jacobian of deformation by gathering the required data from the vision system. Zhang *et al* [283] used real-time FEM simulation using SOFA to predict the Jacobian matrix of the robot. The correct position of the tipping point was modified in the feedback control law using a visual servoing system. Although the vision-based methods are efficient to reduce the number of sensors required to provide the state-space variables of the robots, the hardware requirements and the complex calibration process are the main remaining challenges to using this method in soft robot control scenarios [284, 285].

To summarize this section, figure 9 shows the steps of the SFA fabrication procedure considering all the design parameters, including geometry, materials, constitutive law, and pressure which affect each other during the analysis and manufacturing of soft actuators. It should be noted that selecting the proper material for soft actuators depends on the different factors calculated during analysis.

6. Sensing technology in SFAs

As discussed in the previous section, the modeling and control of SFAs, because of their nonlinear behavior, are generally difficult, and in most cases come with a lot of simplified assumptions. Sensing technology is integrated into SFAs to detect the strain, curvature, contact point, and applied force to facilitate the control process of these kinds of actuators. However, to be integrated into soft actuators, these kinds of sensors must incorporate some special capabilities, such as high stretchability and stiffness, similar to those of the actuator, to prevent any motion restriction. Resistive or capacitive sensors are very popular in force, curvature, or tactile sensing applications. Most of them consist of conductive particles of carbon black [286, 287], graphene [288, 289], metal nanowires, carbon or nano-tubes [290, 291]. McCoul *et al* reviewed other types of electrode materials that are used in stretchable sensors [292]. The main functional difference between the resistive strain and capacitive sensor is that the resistive sensor works by strain changes that alter the conductivity, while the capacitive sensors are dependent on the geometry changes of the area between two electrodes. Yang *et al* [293] printed resistive and capacitive sensors on a paper which was embedded in the SFAs (figure 10(a)).

As they suggested, paper is cheap and can be used as a strain-limiting layer. In some approaches, they integrated commercial flex sensors in the SFAs to measure the bending angle [49, 294]. Kim *et al* [295] compared the performance of two commercial products, Bend Sensor® and Flex Sensor®, to study the bending angle of the finger in hand posture estimation applications. These flex sensors only work in one direction and the results are not accurate when the sensor bends in a different direction. Robinson *et al* [296] demonstrated a highly extensible capacitive sensor that was integrated into SFAs. They use 3D printing to integrate hydrogel electrodes into the silicone. This can also be used as a tactile kinesthetic sensor (figure 10(b)). An optoelectronic sensing method was integrated into SFAs by Zhao *et al* [297]. Its principal functions are based on measuring Lossy waveguides by using a photodetector to specify its deformation, and it

just requires a transparent material to transmit the light. Compared to resistive and capacitive sensors, there is no need to embed conductive materials, and consequently no modification to the stiffness of the actuator. Jung *et al* [298] deployed this kind of sensor to estimate the configuration and shape control of SFAs. To increase optical resolution, the surface of the chamber is coated with a reflective metal layer. As shown in figure 10(c), Truby *et al* [299] proposed 3D printed ionically conductive gels based on resistive sensors and a soft elastomer actuator, which were directly and simultaneously printed. Integrating this sensor on a soft gripper through a multilateral printing platform provides a fully integrated perceptive for haptic sensing applications with closed-loop feedback via curvature, inflation, and contact. The use of a magnetic sensor has recently been reported to indicate SFA curvature [300–302]. The generated output voltage based on the Hall effect is changed due to the position and orientation of the magnet of the Hall element on a flexible circuit. Figure 10(d) shows the developed embedded magnetic curvature sensor in a SFA by Ozel *et al* [303]. Although a magnetic sensor, unlike capacitive and resistive sensors, detects SFA curvature accurately without requiring the application of external forces, adding the magnet and the Hall element affect the stiffness and performance of the actuator. Sensors play a significant role in detecting the behavior of soft actuators, so developments in this area will have promising effects on soft robot actuator applications.

7. Summary and outlook

SFAs were the principal focus of this review study, due to their advantages, including minimal assembly, cost-effectiveness, large deformations, and high generated forces. These capabilities make them suitable for various applications such as gripping, mobility, robotic manipulation, medical tasks, rehabilitation and assistive purposes. We proposed a new general classification of soft pneumatic actuators by considering positive and negative pressure as a power source. We then categorized SFAs based on their design and mechanism into seven classes: Mckibben, continuum robot, PneuNets, universal gripper, origami soft structure, VAMPs and HASEL design. This study provides various information on these well-known approaches, as well as other related works which have been inspired by these effective mechanisms. This classification helps the researcher to present the general kinematic or dynamic modeling or control strategies of each class. In the Hybrid section, the combination of SFAs with other actuating mechanisms is illustrated. This hybrid strategy improves the performance of SFAs with respect to shape configuration, control ability, variable stiffness, and operation range. In SFAs, material selection plays an important role and seems very challenging. Considering this fact, we studied and compared the mechanical properties of the various silicones which are reported in the previous studies. After explaining the different types of modeling and simulation of SFAs, the constitutive materials modeling reported in different articles was reviewed. Toward a better understanding of the differences between the constitutive equations, ABAQUS software was utilized to regenerate the strain-stress data of each article and depicted it in two different graphs, representing engineering strain-stress and true strain-stress for the most popular silicone rubbers. To be more realistic, we selected the Marechal *et al* [245] database as a reference strain-stress database because of its standard procedure of extracting uniaxial tensile stress–strain data. Recent advances in sensor technology in the field of SFAs are illustrated in the sensor section. Finally, two different strategies for SFA fabrication are briefly explained at the end of this study.

Ongoing potential challenges of SFAs in future works can be addressed by improving the controllability of SFAs by embedding distributed sensors. These sensors should measure multi-contact points and simultaneously gather a wide range of object information including surface texture and mass while being stretchable and not increasing the actuators' stiffness. The other critical challenges of SFAs are their portability limitation due to requiring an external source of compressed air, especially for biomimicry applications. Several suggested solutions can be found in the literature but have not been commercialized as of yet. In addition, 3D printing of soft actuators reduces the molding cost and assembly's difficulties of current fabrication methods of SFAs.

Data availability statement

The data that support the findings of this study are available upon reasonable request from the authors.

Acknowledgments

This work was sponsored by the French government research program 'Investissements d'Avenir' through the IDEX-ISITE initiative 16-IDEX-0001 (CAP20-25) and has received funding from the European Union's Horizon 2020 research and innovation program under Grant Agreement No. 869855 (Project SoftManBot). It was also carried out with the support of the Fondation de l'Avenir, Paris, France, 2018, AP-RM-18-020 and the ANR agency (project MANIMAT ANR-20-CE33-0005).

ORCID iDs

Amir Pagoli https://orcid.org/0000-0002-7427-929X
Frédéric Chapelle https://orcid.org/0000-0001-6155-5323

References

[1] Majidi C 2014 Soft robotics: a perspective—current trends and prospects for the future *Soft Robot.* **1** 5–11
[2] Boyraz P, Runge G and Raatz A 2018 An Overview of Novel Actuators for Soft Robotics Actuators *Actuators* vol **7** p 48
[3] Trivedi D, Rahn C D, Kier W M and Walker I D 2008 Soft robotics: biological inspiration, state of the art, and future research *Appl. Bionics Biomech.* **5** 99–117
[4] Rus D and Tolley M T 2015 Design, fabrication and control of soft robots *Nature* **521** 467

[5] Rich S I, Wood R J and Majidi C 2018 Untethered soft robotics *Nat. Electron.* **1** 102

[6] Kim S, Laschi C and Trimmer B 2013 Soft robotics: a bioinspired evolution in robotics *Trends Biotechnol.* **31** 287–94

[7] Laschi C, Mazzolai B and Cianchetti M 2016 Soft robotics: technologies and systems pushing the boundaries of robot abilities *Sci. Robot.* **1** eaah3690

[8] Hughes J, Culha U, Giardina F, Guenther F, Rosendo A and Iida F 2016 Soft manipulators and grippers: a review *Front. Robot.* AI **3** 69

[9] El-Atab N, Mishra R B, Al-Modaf F, Joharji L, Alsharif A A, Alamoudi H, Diaz M, Qaiser N and Hussain M M 2020 Soft actuators for soft robotic applications: a review *Adv. Intell. Syst.* **2** 2000128

[10] Shintake J, Cacucciolo V, Floreano D and Shea H 2018 Soft robotic grippers *Adv. Mater.* **7** 1707035

[11] Gorissen B, Reynaerts D, Konishi S, Yoshida K, Kim J W and De Volder M 2017 Elastic inflatable actuators for soft robotic applications *Adv. Mater.* **29** 1604977

[12] Walker J, Zidek T, Harbel C, Yoon S, Strickland F S, Kumar S and Shin M 2020 Soft Robotics: A Review of Recent Developments of Pneumatic Soft Actuators *Actuators* vol 9 p 3

[13] Hu W, Lum G Z, Mastrangeli M and Sitti M 2018 Small-scale soft-bodied robot with multimodal locomotion *Nature* **554** 81–85

[14] Glick P, Suresh S A, Ruffatto D, Cutkosky M, Tolley M T and Parness A 2018 A soft robotic gripper with gecko-inspired adhesive *IEEE Rob. Autom. Lett.* **3** 903–10

[15] Haines C S, Lima M D, Li N, Spinks G M, Foroughi J, Madden J D, Kim S H, Fang S, De Andrade M J and Göktepe F 2014 Artificial muscles from fishing line and sewing thread *Science* **343** 868–72

[16] Sheng P and Wen W 2012 Electrorheological fluids: mechanisms, dynamics, and microfluidics applications *Annu. Rev. Fluid Mech.* **44** 143–74

[17] Cramer J, Cramer M, Demeester E and Kellens K 2018 exploring the potential of magnetorheology in robotic grippers *Proc. CIRP* **76** 127–32

[18] Geng S, Wang Y, Wang C and Kang R 2018 A space tendon-driven continuum robot **10942** *Int. Conf. on Sensing and Imaging* (Springer) pp 25–35

[19] Shigemune H, Sugano S, Nishitani J, Yamauchi M, Hosoya N, Hashimoto S and Maeda S 2018 Dielectric Elastomer Actuators with Carbon Nanotube Electrodes Painted with a Soft Brush *Actuators* vol **7** p 51

[20] Wang J, Wang Y, Zhu Z, Wang J, He Q and Luo M 2019 The effects of dimensions on the deformation sensing performance of ionic polymer-metal composites *Sensors* **19** 2104

[21] Jani J M, Leary M, Subic A and Gibson M A 2014 A review of shape memory alloy research, applications and opportunities *Mater. Design* **56** 1078–113

[22] Lendlein A and Kelch S 2002 Shape-memory polymers *Angew. Chem., Int. Ed. Engl.* **41** 2034–57

[23] Fatahillah M, Oh N and Rodrigue H 2020 A novel soft bending actuator using combined positive and negative pressures *Front. Bioeng. Biotechnol.* **8** 472

[24] Singh P K and Krishna C M 2014 Continuum arm robotic manipulator: a review *Univ. J. Mech. Eng.* **2** 193–8

[25] Ouyang B, Liu Y and Sun D 2016 Design of a three-segment continuum robot for minimally invasive surgery *Rob. Biomimetics* **3** 1–4

[26] Walker I D 2013 Continuous Backbone "Continuum" Robot Manipulators *International Scholarly Research Notices* vol 1–19

[27] Romasanta L J, López-Manchado M A and Verdejo R 2015 Increasing the performance of dielectric elastomer actuators: a review from the materials perspective *Prog. Polym. Sci.* **51** 188–211

[28] Brochu P and Pei Q 2012 Dielectric elastomers for actuators and artificial muscles *Electroactivity in Polymeric Materials* (Berlin: Springer) pp 1–56

[29] Maffli L, Rosset S, Ghilardi M, Carpi F and Shea H 2015 Ultrafast all-polymer electrically tunable silicone lenses *Adv. Funct. Mater.* **25** 1656–65

[30] Jung K, Koo J C, Nam J-D, Lee Y K and Choi H R 2007 Artificial annelid robot driven by soft actuators *Bioinspir. Biomim.* **2** S42

[31] Rendl C, Kim D, Fanello S, Parzer P, Rhemann C, Taylor J, Zirkl M, Scheipl G, Rothländer T and Haller M 2014 FlexSense: a transparent self-sensing deformable surface *Proc. of the 27th Annual ACM Symp. on User Interface Software and Technology* pp 129–38

[32] Rizzello G, Naso D, York A and Seelecke S 2016 Closed loop control of dielectric elastomer actuators based on self-sensing displacement feedback *Smart Mater. Struct.* **25** 035034

[33] Gupta U, Qin L, Wang Y, Godaba H and Zhu J 2019 Soft robots based on dielectric elastomer actuators: a review *Smart Mater. Struct.* **28** 103002

[34] Lee C, Kim M, Kim Y J, Hong N, Ryu S, Kim H J and Kim S 2017 Soft robot review *Int. J. Control Autom. Syst.* **15** 3–15

[35] Anderson I A, Gisby T A, McKay T G, O'Brien B M and Calius E P 2012 Multi-functional dielectric elastomer artificial muscles for soft and smart machines *J. Appl. Phys.* **112** 041101

[36] Araromi O A, Gavrilovich I, Shintake J, Rosset S, Richard M, Gass V and Shea H R 2014 Rollable multisegment dielectric elastomer minimum energy structures for a deployable microsatellite gripper *IEEE/ASME Trans. Mechatron.* **20** 438–46

[37] Heng K-R, Ahmed A S, Shrestha M and Lau G-K 2017 Strong dielectric-elastomer grippers with tension arch flexures *Electroactive Polymer Actuators and Devices (EAPAD) 2017* vol 10163 (International Society for Optics and Photonics) p 101631Z

[38] O'Halloran A, O'malley F and McHugh P 2008 A review on dielectric elastomer actuators, technology, applications, and challenges *J. Appl. Phys.* **104** 9

[39] Mardani A, Zavadskas E K, Streimikiene D, Jusoh A and Khoshnoudi M 2017 A comprehensive review of data envelopment analysis (DEA) approach in energy efficiency *Renew. Sustain. Energy Rev.* **70** 1298–322

[40] Cook W D, Liang L and Zhu J 2010 Measuring performance of two-stage network structures by DEA: a review and future perspective *Omega* **38** 423–30

[41] Poulin A, Rosset S and Shea H R 2015 Printing low-voltage dielectric elastomer actuators *Appl. Phys. Lett.* **107** 244104

[42] Ji X, Liu X, Cacucciolo V, Imboden M, Civet Y, El Haitami A, Cantin S, Perriard Y and Shea H 2019 An autonomous untethered fast soft robotic insect driven by low-voltage dielectric elastomer actuators *Sci. Robot.* **4** 1707035

[43] Kussmaul B, Risse S, Kofod G, Waché R, Wegener M, McCarthy D N, Krüger H and Gerhard R 2011 Enhancement of dielectric permittivity and electromechanical response in silicone elastomers: molecular grafting of organic dipoles to the macromolecular network *Adv. Funct. Mater.* **21** 4589–94

[44] Yang D, Ge F, Tian M, Ning N, Zhang L, Zhao C, Ito K, Nishi T, Wang H and Luan Y 2015 Dielectric elastomer actuator with excellent electromechanical performance

using slide-ring materials/barium titanate composites *J. Mater. Chem.* A **3** 9468–79
[45] Madsen F B, Daugaard A E, Hvilsted S and Skov A L 2016 The current state of silicone-based dielectric elastomer transducers *Macromol. Rapid Commun.* **37** 378–413
[46] Kashmery H A 2019 Polyvinylidene fluoride/sulfonated graphene oxide blend membrane coated with polypyrrole/platinum electrode for ionic polymer metal composite actuator applications *Sci. Rep.* **9** 1–11
[47] Cianchetti M, Licofonte A, Follador M, Rogai F and Laschi C 2014 Bioinspired Soft Actuation System Using Shape Memory Alloys *Actuators* vol 3 pp 226–44
[48] Ge Q, Sakhaei A H, Lee H, Dunn C K, Fang N X and Dunn M L 2016 Multimaterial 4D printing with tailorable shape memory polymers *Sci. Rep.* **6** 31110
[49] Elgeneidy K, Lohse N and Jackson M 2018 Bending angle prediction and control of soft pneumatic actuators with embedded flex sensors–a data-driven approach *Mechatronics* **50** 234–47
[50] Vikas V, Cohen E, Grassi R, Sözer C and Trimmer B 2016 Design and locomotion control of a soft robot using friction manipulation and motor–tendon actuation *IEEE Trans. Robot.* **32** 949–59
[51] Chirikjian G S 2015 Conformational modeling of continuum structures in robotics and structural biology: a review *Adv. Robot.* **29** 817–29
[52] Chirikjian G S and Burdick J W 1995 Kinematically optimal hyper-redundant manipulator configurations *IEEE Trans. Robot. Autom.* **11** 794–806
[53] Hannan M W and Walker I D 2003 Kinematics and the implementation of an elephant's trunk manipulator and other continuum style robots *J. Robot. Syst.* **20** 45–63
[54] Jones B A and Walker I D 2006 Kinematics for multisection continuum robots *IEEE Trans. Robot.* **22** 43–55
[55] Simaan N 2005 Snake-like units using flexible backbones and actuation redundancy for enhanced miniaturization *Proc. of the 2005 IEEE Int. Conf. on Robotics and Automation* (IEEE) pp 3012–7
[56] Xu K and Simaan N 2006 Actuation compensation for flexible surgical snake-like robots with redundant remote actuation *Proc. 2006 IEEE Int. Conf. on Robotics and Automation, 2006. ICRA 2006.* (IEEE) pp 4148–54
[57] Webster III R J and Jones B A 2010 Design and kinematic modeling of constant curvature continuum robots: a review *Int. J. Rob. Res.* **29** 1661–83
[58] Shahinpoor M, Kim K J and Leo D J 2003 Ionic polymer-metal composites as multifunctional materials *Polym. Compos.* **24** 24–33
[59] Li W B, Zhang W M, Zou H X, Peng Z K and Meng G 2018 A fast rolling soft robot driven by dielectric elastomer *IEEE/ASME Trans. Mechatron.* **23** 1630–40
[60] Kim K J and Tadokoro S 2007 *Electroactive Polymers for Robotic Applications: Artificial Muscles and Sensors* (London: Springer) 291
[61] Pelrine R, Kornbluh R D, Eckerle J, Jeuck P, Oh S, Pei Q and Stanford S 2001 Dielectric elastomers: generator mode fundamentals and applications *Smart Structures and Materials 2001: Electroactive Polymer Actuators and Devices* (International Society for Optics and Photonics) vol 4329 pp 148–56
[62] Keplinger C, Li T, Baumgartner R, Suo Z and Bauer S 2012 Harnessing snap-through instability in soft dielectrics to achieve giant voltage-triggered deformation *Soft Matter* **8** 285–8
[63] Gu G-Y, Zhu J, Zhu L-M and Zhu X 2017 A survey on dielectric elastomer actuators for soft robots *Bioinspir. Biomim.* **12** 011003
[64] Acome E, Mitchell S K, Morrissey T G, Emmett M B, Benjamin C, King M, Radakovitz M and Keplinger C 2018 Hydraulically amplified self-healing electrostatic actuators with muscle-like performance *Science* **359** 61–65
[65] Cheng X, Yu M, Ma J, Li B, Zhang Y, Wang P and Jiao Z 2020 An entirely soft varifocal lens based on an electro-hydraulic actuator *Smart Mater. Struct.* **29** 045017
[66] Schunk C, Pearson L, Acome E, Morrissey T G, Correll N, Keplinger C, Rentschler M E and Humbert J S 2018 System identification and closed-loop control of a hydraulically amplified self-healing electrostatic (HASEL) actuator *2018 IEEE/RSJ Int. Conf. on Intelligent Robots and Systems (IROS) Madrid, Spain* (IEEE) pp 6417–23
[67] Rothemund P, Kellaris N, Mitchell S K, Acome E and Keplinger C 2020 HASEL artificial muscles for a new generation of lifelike robots—recent progress and future opportunities *Adv. Mater.* **33** 2003375
[68] Marette A, Poulin A, Besse N, Rosset S, Briand D and Shea H 2017 Flexible zinc–tin oxide thin film transistors operating at 1 kV for integrated switching of dielectric elastomer actuators arrays *Adv. Mater.* **29** 1700880
[69] Kellaris N, Venkata V G, Smith G M, Mitchell S K and Keplinger C 2018 Peano-HASEL actuators: muscle-mimetic, electrohydraulic transducers that linearly contract on activation *Sci. Robot.* **3**
[70] Oguro K 1992 Bending of an ion-conducting polymer film-electrode composite by an electric stimulus at low voltage *J. Micromach. Soc.* **5** 27–30
[71] Shahinpoor M and Kim K J 2001 Ionic polymer-metal composites: i. Fundamentals *Smart Mater. Struct.* **10** 819
[72] Kim K J and Shahinpoor M 2003 Ionic polymer–metal composites: II. Manufacturing techniques *Smart Mater. Struct.* **12** 65
[73] Shahinpoor M and Kim K J 2004 Ionic polymer–metal composites: III. Modeling and simulation as biomimetic sensors, actuators, transducers, and artificial muscles *Smart Mater. Struct.* **13** 1362
[74] Shahinpoor M and Kim K J 2004 Ionic polymer–metal composites: IV. Industrial and medical applications *Smart Mater. Struct.* **14** 197
[75] Tiwari R and Garcia E 2011 The state of understanding of ionic polymer metal composite architecture: a review *Smart Mater. Struct.* **20** 083001
[76] Bhandari B, Lee G-Y and Ahn S-H 2012 A review on IPMC material as actuators and sensors: fabrications, characteristics and applications *Int. J. Precis. Eng. Manuf.* **13** 141–63
[77] Jo C, Pugal D, Oh I-K, Kim K J and Asaka K 2013 Recent advances in ionic polymer–metal composite actuators and their modeling and applications *Prog. Polym. Sci.* **38** 1037–66
[78] Hao M, Wang Y, Zhu Z, He Q, Zhu D and Luo M 2019 A compact review of IPMC as soft actuator and sensor: current trends, challenges, and potential solutions from our recent work *Front. Robot.* AI **6** 129
[79] Otsuka K and Wayman C M 1999 *Shape Memory Materials* (Cambridge: Cambridge University)
[80] Ozbulut O E, Daghash S and Sherif M M 2016 Shape memory alloy cables for structural applications *J. Mater. Civil Eng.* **28** 04015176
[81] Rodrigue H, Wang W, Han M-W, Kim T J and Ahn S-H 2017 An overview of shape memory alloy-coupled actuators and robots *Soft Robot.* **4** 3–15
[82] Behl M and Lendlein A 2007 Shape-memory polymers **10** 20–28
[83] Hager M D, Bode S, Weber C and Schubert U S 2015 Shape memory polymers: past, present and future developments *Prog. Polym. Sci.* **49** 3–33
[84] Behl M, Kratz K, Zotzmann J, Nöchel U and Lendlein A 2013 Reversible bidirectional shape-memory polymers *Adv. Mater.* **25** 4466–9

[85] Wang W and Ahn S-H 2017 Shape memory alloy-based soft gripper with variable stiffness for compliant and effective grasping *Soft Robot.* **4** 379–89

[86] Yang Y, Chen Y, Li Y, Chen M Z and Wei Y 2017 Bioinspired robotic fingers based on pneumatic actuator and 3D printing of smart material *Soft Robot.* **4** 147–62

[87] Lendlein A, Behl M, Hiebl B and Wischke C 2010 Shape-memory polymers as a technology platform for biomedical applications *Expert Rev. Med. Devices* **7** 357–79

[88] Meng H and Li G 2013 A review of stimuli-responsive shape memory polymer composites *Polymer* **54** 2199–221

[89] Krieger Y S, Schiele S, Detzel S, Dietz C and Lueth T C 2019 Shape memory structures-automated design of monolithic soft robot structures with pre-defined end poses *2019 Int. Conf. on Robotics and Automation (ICRA)* (IEEE) pp 9357–62

[90] Marchese A D and Rus D 2016 Design, kinematics, and control of a soft spatial fluidic elastomer manipulator *Int. J. Robot. Res.* **35** 840–69

[91] Park W, Seo S, Oh J and Bae J 2020 A sensorized hybrid gripper to evaluate a grasping quality based on a largest minimum wrench *IEEE Rob. Autom. Lett.* **5** 3243–50

[92] Zhou J, Chen X, Li J, Tian Y and Wang Z 2018 A soft robotic approach to robust and dexterous grasping *2018 IEEE Int. Conf. on Soft Robotics (Robosoft)* (IEEE) pp 412–7

[93] Nakajima T, Yamaguchi T, Wakabayashi S, Arie T, Akita S and Takei K 2020 Transformable pneumatic balloon-type soft robot using attachable shells *Adv. Mater. Technol.* **5** 2000201

[94] Shepherd R F, Ilievski F, Choi W, Morin S A, Stokes A A, Mazzeo A D, Chen X, Wang M and Whitesides G M 2011 Multigait soft robot *Proc. Natl Acad. Sci.* **108** 20400–3

[95] McMahan W, Chitrakaran V, Csencsits M, Dawson D, Walker I D, Jones B A, Pritts M, Dienno D, Grissom M and Rahn C D 2006 Field trials and testing of the OctArm continuum manipulator *Proc. 2006 IEEE Int. Conf. on Robotics and Automation, 2006. ICRA 2006.* (IEEE) pp 2336–41

[96] Abondance S, Teeple C B and Wood R J 2020 A dexterous soft robotic hand for delicate in-hand manipulation *IEEE Robot. Autom. Lett.* **5** 5502–9

[97] Heo S-H, Kim C, Kim T-S and Park H-S 2020 Human-palm-inspired artificial skin material enhances operational functionality of hand manipulation *Adv. Funct. Mater.* **30** 2002360

[98] Cianchetti M, Ranzani T, Gerboni G, De Falco I, Laschi C and Menciassi A 2013 STIFF-FLOP surgical manipulator: mechanical design and experimental characterization of the single module *Intelligent Robots and Systems (IROS), 2013 IEEE/RSJ Int. Conf. On* (IEEE) pp 3576–81

[99] Abidi H, Gerboni G, Brancadoro M, Fras J, Diodato A, Cianchetti M, Wurdemann H, Althoefer K and Menciassi A 2018 Highly dexterous 2-module soft robot for intra-organ navigation in minimally invasive surgery *Int. J. Med. Robot. Comput. Assisted Surg.* **14** e1875

[100] Polygerinos P, Wang Z, Galloway K C, Wood R J and Walsh C J 2015 Soft robotic glove for combined assistance and at-home rehabilitation *Robot. Auton. Syst.* **73** 135–43

[101] Yap H K, Lim J H, Nasrallah F, Goh J C and Yeow R C 2015 A soft exoskeleton for hand assistive and rehabilitation application using pneumatic actuators with variable stiffness *2015 IEEE Int. Conf. on Robotics and Automation (ICRA)* (IEEE) pp 4967–72

[102] Yap H K, Ng H Y and Yeow C-H 2016 High-force soft printable pneumatics for soft robotic applications *Soft Robot.* **3** 144–58

[103] Bao G, Fang H, Chen L, Wan Y, Xu F, Yang Q and Zhang L 2018 Soft robotics: academic insights and perspectives through bibliometric analysis *Soft Robot.* **5** 229–41

[104] Suzumori K, Iikura S and Tanaka H 1991 Development of flexible microactuator and its applications to robotic mechanisms *Proc.. 1991 IEEE Int. Conf. on Robotics and Automation* (IEEE Computer Society) pp 1622–3

[105] Xing K, Wang Y, Zhu Q and Zhou H 2012 Modeling and control of McKibben artificial muscle enhanced with echo state networks *Control Eng. Pract.* **20** 477–88

[106] Grissom M D, Chitrakaran V, Dienno D, Csencits M, Pritts M, Jones B, McMahan W, Dawson D, Rahn C and Walker I 2006 Design and experimental testing of the octarm soft robot manipulator *Unmanned Systems Technology VIII* vol **6230** (International Society for Optics and Photonics) p 62301F

[107] Ilievski F, Mazzeo A D, Shepherd R F, Chen X and Whitesides G M 2011 Soft robotics for chemists *Angew. Chem.* **123** 1930–5

[108] Brown E, Rodenberg N, Amend J, Mozeika A, Steltz E, Zakin M R, Lipson H and Jaeger H M 2010 Universal robotic gripper based on the jamming of granular material *Proc. Natl Acad. Sci.* **107** 18809–14

[109] Martinez R V, Fish C R, Chen X and Whitesides G M 2012 Elastomeric origami: programmable paper-elastomer composites as pneumatic actuators *Adv. Funct. Mater.* **22** 1376–84

[110] Yang D, Verma M S, So J-H, Mosadegh B, Keplinger C, Lee B, Khashai F, Lossner E, Suo Z and Whitesides G M 2016 Buckling pneumatic linear actuators inspired by muscle *Adv. Mater. Technol.* **1** 1600055

[111] Mitchell S K, Wang X, Acome E, Martin T, Ly K, Kellaris N, Venkata V G and Keplinger C 2019 An easy-to-implement toolkit to create versatile and high-performance HASEL actuators for untethered soft robots *Adv. Sci.* **6** 1900178

[112] Daerden F and Lefeber D 2002 Pneumatic artificial muscles: actuators for robotics and automation *Eur. J. Mech. Environ. Eng.* **47** 11–21

[113] Tondu B 2012 Modelling of the McKibben artificial muscle: a review *J. Intell. Mater. Syst. Struct.* **23** 225–53

[114] Al Abeach L A, Nefti-Meziani S and Davis S 2017 Design of a variable stiffness soft dexterous gripper *Soft Robot.* **4** 274–84

[115] Gomez M, Moulton D E and Vella D 2017 Critical slowing down in purely elastic 'snap-through'instabilities *Nat. Phys.* **13** 142–5

[116] Overvelde J T, Kloek T, D'haen J J and Bertoldi K 2015 Amplifying the response of soft actuators by harnessing snap-through instabilities *Proc. Natl Acad. Sci.* **112** 10863–8

[117] Tsukagoshi H, Kitagawa A and Segawa M 2001 Active hose: an artificial elephant's nose with maneuverability for rescue operation *Proc. 2001 ICRA. IEEE Int. Conf. on Robotics and Automation (Cat. No. 01CH37164)* vol **3** (IEEE) pp 2454–9

[118] Walker I D, Dawson D M, Flash T, Grasso F W, Hanlon R T, Hochner B, Kier W M, Pagano C C, Rahn C D and Zhang Q M 2005 Continuum robot arms inspired by cephalopods *Unmanned Ground Vehicle Technology VII* vol **5804** (International Society for Optics and Photonics) pp 303–14

[119] Kang R, Branson D T, Zheng T, Guglielmino E and Caldwell D G 2013 Design, modeling and control of a pneumatically actuated manipulator inspired by biological continuum structures *Bioinspir. Biomim.* **8** 036008

[120] Suzumori K, Iikura S and Tanaka H 1992 Applying a flexible microactuator to robotic mechanisms *IEEE Control Syst. Mag.* **12** 21–27

[121] Onal C D, Chen X, Whitesides G M and Rus D 2017 Soft mobile robots with on-board chemical pressure generation *Robotics Research* (Berlin: Springer) pp 525–40

[122] Katzschmann R K, Marchese A D and Rus D 2016 Hydraulic autonomous soft robotic fish for 3D swimming *Experimental Robotics* (Berlin: Springer) pp 405–20

[123] Sridar S, Majeika C J, Schaffer P, Bowers M, Ueda S, Barth A J, Sorrells J L, Wu J T, Hunt T R and Popovic M 2016 Hydro Muscle-a novel soft fluidic actuator *2016 IEEE Int. Conf. on Robotics and Automation (ICRA)* (IEEE) pp 4014–21

[124] Yuk H, Lin S, Ma C, Takaffoli M, Fang N X and Zhao X 2017 Hydraulic hydrogel actuators and robots optically and sonically camouflaged in water *Nat. Commun.* **8** 1–12

[125] Miron G, Bédard B and Plante J-S 2018 Sleeved Bending Actuators for Soft Grippers: A Durable Solution for High Force-to-Weight Applications *Actuators* vol **7** pp 40

[126] Mosadegh B, Polygerinos P, Keplinger C, Wennstedt S, Shepherd R F, Gupta U, Shim J, Bertoldi K, Walsh C J and Whitesides G M 2014 Pneumatic networks for soft robotics that actuate rapidly *Adv. Funct. Mater.* **24** 2163–70

[127] Veale A J, Xie S Q and Anderson I A 2016 Characterizing the Peano fluidic muscle and the effects of its geometry properties on its behavior *Smart Mater. Struct.* **25** 065013

[128] Rothemund P, Ainla A, Belding L, Preston D J, Kurihara S, Suo Z and Whitesides G M 2018 A soft, bistable valve for autonomous control of soft actuators *Sci. Robot.* **3**

[129] Tolley M T, Shepherd R F, Mosadegh B, Galloway K C, Wehner M, Karpelson M, Wood R J and Whitesides G M 2014 A resilient, untethered soft robot *Soft Robot.* **1** 213–23

[130] Needleman A 1977 Inflation of spherical rubber balloons *Int. J. Solids Struct.* **13** 409–21

[131] Shepherd R F, Stokes A A, Nunes R M and Whitesides G M 2013 Soft machines that are resistant to puncture and that self seal *Adv. Mater.* **25** 6709–13

[132] Deimel R and Brock O 2013 A compliant hand based on a novel pneumatic actuator *2013 IEEE Int. Conf. on Robotics and Automation* (IEEE) pp 2047–53

[133] Deimel R and Brock O 2016 A novel type of compliant and underactuated robotic hand for dexterous grasping *Int. J. Robot. Res.* **35** 161–85

[134] Veale A J, Xie S Q and Anderson I A 2016 Modeling the Peano fluidic muscle and the effects of its material properties on its static and dynamic behavior *Smart Mater. Struct.* **25** 065014

[135] Veale A J, Xie S Q and Anderson I A 2018 Accurate multivariable arbitrary piecewise model regression of McKibben and Peano muscle static and damping force behavior *Smart Mater. Struct.* **27** 105048

[136] Wang X, Mitchell S K, Rumley E H, Rothemund P and Keplinger C 2020 High-strain peano-HASEL actuators *Adv. Funct. Mater.* **30** 1908821

[137] Yoder Z, Kellaris N, Chase-Markopoulou C, Ricken D, Mitchell S K, Emmett M B, Segil J and Keplinger C 2020 Design of a high-speed prosthetic finger driven by peano-HASEL actuators *Front. Robot.* AI **7** 181

[138] Amend J, Cheng N, Fakhouri S and Culley B 2016 Soft robotics commercialization: jamming grippers from research to product *Soft Robot.* **3** 213–22

[139] Cheng N, Amend J, Farrell T, Latour D, Martinez C, Johansson J, McNicoll A, Wartenberg M, Naseef S and Hanson W 2016 Prosthetic jamming terminal device: a case study of untethered soft robotics *Soft Robot.* **3** 205–12

[140] Reitelshöfer S, Ramer C, Gräf D, Matern F and Franke J 2014 Combining a collaborative robot and a lightweight Jamming-Gripper to realize an intuitively to use and flexible co-worker *2014 IEEE/SICE Int. Symp. on System Integration* (IEEE) pp 1–5

[141] Harada K, Nagata K, Rojas J, Ramirez-Alpizar I G, Wan W, Onda H and Tsuji T 2016 Proposal of a shape adaptive gripper for robotic assembly tasks *Adv. Robot.* **30** 1186–98

[142] Licht S, Collins E, Mendes M L and Baxter C 2017 Stronger at depth: jamming grippers as deep sea sampling tools *Soft Robot.* **4** 305–16

[143] Loeve A J, van de Ven O S, Vogel J G, Breedveld P and Dankelman J 2010 Vacuum packed particles as flexible endoscope guides with controllable rigidity *Granular Matter* **12** 543–54

[144] De Falco I, Cianchetti M and Menciassi A 2017 A soft multi-module manipulator with variable stiffness for minimally invasive surgery *Bioinspir. Biomim.* **12** 056008

[145] Amend J and Lipson H 2017 The JamHand: dexterous manipulation with minimal actuation *Soft Robot.* **4** 70–80

[146] Robertson M A and Paik J 2017 New soft robots really suck: vacuum-powered systems empower diverse capabilities *Sci. Robot.* **2** eaan6357

[147] Follmer S, Leithinger D, Olwal A, Cheng N and Ishii H 2012 Jamming user interfaces: programmable particle stiffness and sensing for malleable and shape-changing devices *Proc. of the 25th Annual ACM Symp. on User Interface Software and Technology (ACM)* pp 519–28

[148] Jiang A, Xynogalas G, Dasgupta P, Althoefer K and Nanayakkara T 2012 Design of a variable stiffness flexible manipulator with composite granular jamming and membrane coupling *Intelligent Robots and Systems (IROS), 2012 IEEE/RSJ Int. Conf. On* (IEEE) pp 2922–7

[149] Sayyadan S M Z and Moniri M M 2018 Mechanical behaviors of jammable robotic structures; prediction and computation *Int. J. Intell. Robot. Appl.* **3** 1–16

[150] Yang D, Verma M S, Lossner E, Stothers D and Whitesides G M 2017 Negative-pressure soft linear actuator with a mechanical advantage *Adv. Mater. Technol.* **2** 1600164

[151] Jiao Z, Ji C, Zou J, Yang H and Pan M 2019 Vacuum-powered soft pneumatic twisting actuators to empower new capabilities for soft robots *Adv. Mater. Technol.* **4** 1800429

[152] Chen R, Zhang C, Sun Y, Yu T, Shen X-M, Yuan Z-A and Guo J-L 2021 A paper fortune teller-inspired reconfigurable soft pneumatic gripper *Smart Mater. Struct.* **30** 045002

[153] Lee J-G and Rodrigue H 2019 Efficiency of origami-based vacuum pneumatic artificial muscle for off-grid operation *Int. J. Precis. Eng. Manuf. Green Technol.* **6** 789–97

[154] Verma M S, Ainla A, Yang D, Harburg D and Whitesides G M 2018 A soft tube-climbing robot *Soft Robot.* **5** 133–7

[155] Demaine E D and O'Rourke J 2007 *Geometric Folding Algorithms: Linkages, Origami, Polyhedra* (Cambridge: Cambridge university)

[156] Li S, Vogt D M, Rus D and Wood R J 2017 Fluid-driven origami-inspired artificial muscles *Proc. Natl Acad. Sci.* **114** 13132–7

[157] Li J, Godaba H, Zhang Z Q, Foo C C and Zhu J 2018 A soft active origami robot *Extreme Mech. Lett.* **24** 30–37

[158] Paez L, Agarwal G and Paik J 2016 Design and analysis of a soft pneumatic actuator with origami shell reinforcement *Soft Robot.* **3** 109–19

[159] Rus D and Tolley M T 2018 Design, fabrication and control of origami robots *Nat. Rev. Mater.* **3** 101–12

[160] Yang Y, Chen Y, Li Y, Wang Z and Li Y 2017 Novel variable-stiffness robotic fingers with built-in position feedback *Soft Robot.* **4** 338–52

[161] Hao Y, Wang T, Xie Z, Sun W, Liu Z, Fang X, Yang M and Wen L 2018 A eutectic-alloy-infused soft actuator with sensing, tunable degrees of freedom, and stiffness properties *J. Micromech. Microeng.* **28** 024004

[162] Narang Y S, Vlassak J J and Howe R D 2018 Mechanically versatile soft machines through laminar jamming *Adv. Funct. Mater.* **28** 1707136

[163] Yang Y, Zhang Y, Kan Z, Zeng J and Wang M Y 2020 Hybrid jamming for bioinspired soft robotic fingers *Soft Robot.* **7** 292–308

[164] Guo J, Elgeneidy K, Xiang C, Lohse N, Justham L and Rossiter J 2018 Soft pneumatic grippers embedded with stretchable electroadhesion *Smart Mater. Struct.* **27** 055006

[165] Kim Y and Cha Y 2020 Soft pneumatic gripper with a tendon-driven soft origami pump *Front. Bioeng. Biotechnol.* **8** 461

[166] Anon Mold making & casting materials | rubbers, plastics, foams & more! *Smooth-On, Inc*

[167] Anon SYLGARD^{TM} 184 silicone elastomer kit | dow Inc

[168] Anon ELASTOSIL$^{®}$ M 4601 A/B | room temperature curing silicone rubber (RTV-2) | wacker chemie AG *WACKER Website*

[169] Yildiz S K, Mutlu R and Alici G 2016 Fabrication and characterisation of highly stretchable elastomeric strain sensors for prosthetic hand applications *Sens. Actuators* A **247** 514–21

[170] Park Y-L, Majidi C, Kramer R, Bérard P and Wood R J 2010 Hyperelastic pressure sensing with a liquid-embedded elastomer *J. Micromech. Microeng.* **20** 125029

[171] Kwon D, Lee T-I, Shim J, Ryu S, Kim M S, Kim S, Kim T-S and Park I 2016 Highly sensitive, flexible, and wearable pressure sensor based on a giant piezocapacitive effect of three-dimensional microporous elastomeric dielectric layer *ACS Appl. Mater. Interfaces* **8** 16922–31

[172] Yeo J C and Lim C T 2016 Emerging flexible and wearable physical sensing platforms for healthcare and biomedical applications *Microsyst. Nanoeng.* **2** 1–19

[173] Mai H, Mutlu R, Tawk C, Alici G and Sencadas V 2019 Ultra-stretchable MWCNT–Ecoflex piezoresistive sensors for human motion detection applications *Compos. Sci. Technol.* **173** 118–24

[174] Elsayed Y, Vincensi A, Lekakou C, Geng T, Saaj C M, Ranzani T, Cianchetti M and Menciassi A 2014 Finite element analysis and design optimization of a pneumatically actuating silicone module for robotic surgery applications *Soft Robot.* **1** 255–62

[175] Calisti M, Arienti A, Renda F, Levy G, Hochner B, Mazzolai B, Dario P and Laschi C 2012 Design and development of a soft robot with crawling and grasping capabilities *2012 IEEE Int. Conf. on Robotics and Automation* (IEEE) pp 4950–5

[176] Tian M, Xiao Y, Wang X, Chen J and Zhao W 2017 Design and experimental research of pneumatic soft humanoid robot hand *Robot Intelligence Technology and Applications* vol 4 (Berlin: Springer) pp 469–78

[177] Yang Y and Chen Y 2017 3D printing of smart materials for robotics with variable stiffness and position feedback *2017 IEEE Int. Conf. on Advanced Intelligent Mechatronics (AIM)* (IEEE) pp 418–23

[178] Yoshida S, Morimoto Y, Zheng L, Onoe H and Takeuchi S 2018 Multipoint bending and shape retention of a pneumatic bending actuator by a variable stiffness endoskeleton *Soft Robot.* **5** 718–25

[179] Pourazadi S, Bui H and Menon C 2019 Investigation on a soft grasping gripper based on dielectric elastomer actuators *Smart Mater. Struct.* **28** 035009

[180] Luo M, Liu L, Liu C, Li B, Cao C, Gao X and Li D 2020 A single-chamber pneumatic soft bending actuator with increased stroke-range by local electric guidance *IEEE Trans. Ind. Electron.* 8455–63

[181] Li Y, Chen Y, Ren T, Li Y and Choi S H 2018 Precharged pneumatic soft actuators and their applications to untethered soft robots *Soft Robot.* **5** 567–75

[182] Pagoli A, Chapelle F, Ramon J A C, Mezouar Y and Lapusta Y 2020 Design and optimization of a dextrous robotic finger: incorporating a sliding, rotating, and soft-bending mechanism while maximizing dexterity and minimizing dimensions *IEEE Robot. Autom. Mag.* **27** 56–64

[183] Pagoli A, Chapelle F, Ramon J A C, Mezouar Y and Lapusta Y 2021 A soft robotic gripper with an active palm and reconfigurable fingers for fully dexterous in-hand manipulation *IEEE Robot. Autom. Lett.* **6** 7706–13

[184] Stokes A A, Shepherd R F, Morin S A, Ilievski F and Whitesides G M 2014 A hybrid combining hard and soft robots *Soft Robot.* **1** 70–74

[185] Li Y, Chen Y and Li Y 2018 Distributed design of passive particle jamming based soft grippers *2018 IEEE Int. Conf. on Soft Robotics (Robosoft)* (IEEE) pp 547–52

[186] Chen Y, Li Y, Li Y and Wang Y 2017 Stiffening of soft robotic actuators—Jamming approaches *2017 IEEE Int. Conf. on Real-time Computing and Robotics (RCAR)* (IEEE) pp 17–21

[187] Yu M, Yang W, Yu Y, Cheng X and Jiao Z 2020 A Crawling Soft Robot Driven by Pneumatic Foldable Actuators Based on Miura-Ori *Actuators* vol **9** p 26

[188] Seibel A and Yıldız M 2020 A gecko-inspired soft passive gripper *Biomimetics* **5** 12

[189] Anon Silane, silicone & metal-organic materials innovation (Gelest)

[190] Yap H K, Lim J H, Nasrallah F, Cho Hong Goh J and Yeow C-H 2016 Characterisation and evaluation of soft elastomeric actuators for hand assistive and rehabilitation applications *J. Med. Eng. Technol.* **40** 199–209

[191] Anon momentive *MPMSitefinityCMS*

[192] Anon Shin-etsu silicone : offering a variety of silicone to industrial fields

[193] Anon Recreus filaflex | 3D printing | 3D filament sale *recreus*

[194] Anon NinjaTek | ninjaFlex material is the leading flexible filament in the 3D printing industry

[195] Anon Stratasys: 3D printing & additive manufacturing *stratasys*

[196] Park S, Mondal K, Treadway III R M, Kumar V, Ma S, Holbery J D and Dickey M D 2018 Silicones for stretchable and durable soft devices: beyond sylgard-184 *ACS Appl. Mater. Interfaces* **10** 11261–8

[197] Anon Dow | the materials science company | explore products

[198] Shintake J, Rosset S, Schubert B, Mintchev S, Floreano D and Shea H 2015 DEA for soft robotics: 1-gram actuator picks up a 60-gram egg *Electroactive Polymer Actuators and Devices (EAPAD) 2015* vol 9430 (International Society for Optics and Photonics) p 94301S

[199] Alizadehyazdi V, Bonthron M and Spenko M 2020 An electrostatic/gecko-inspired adhesives soft robotic gripper *IEEE Robot. Autom. Lett.* **5** 4679–86

[200] Cai L, Song L, Luan P, Zhang Q, Zhang N, Gao Q, Zhao D, Zhang X, Tu M and Yang F 2013 Super-stretchable, transparent carbon nanotube-based capacitive strain sensors for human motion detection *Sci. Rep.* **3** 3048

[201] Woo S-J, Kong J-H, Kim D-G and Kim J-M 2014 A thin all-elastomeric capacitive pressure sensor array based on micro-contact printed elastic conductors *J. Mater. Chem.* C **2** 4415–22
[202] Lee H-K, Chang S-I and Yoon E 2006 A flexible polymer tactile sensor: fabrication and modular expandability for large area deployment *J. Microelectromech. Syst.* **15** 1681–6
[203] White E L, Case J C and Kramer R K 2017 Multi-mode strain and curvature sensors for soft robotic applications *Sens. Actuators* A **253** 188–97
[204] Markvicka E J, Tutika R, Bartlett M D and Majidi C 2019 Soft electronic skin for multi-site damage detection and localization *Adv. Funct. Mater.* **29** 1900160
[205] Tang W, Zhang C, Zhong Y, Zhu P, Hu Y, Jiao Z, Wei X, Lu G, Wang J and Liang Y 2021 Customizing a self-healing soft pump for robot *Nat. Commun.* **12** 1–11
[206] Huynh T-P, Sonar P and Haick H 2017 Advanced materials for use in soft self-healing devices *Adv. Mater.* **29** 1604973
[207] Terryn S, Mathijssen G, Brancart J, Van Assche G, Vanderborght B and Lefeber D 2015 Investigation of self-healing compliant actuators for robotics *2015 IEEE Int. Conf. on Robotics and Automation (ICRA)* (IEEE) pp 258–63
[208] Terryn S, Brancart J, Lefeber D, Van Assche G and Vanderborght B 2017 Self-healing soft pneumatic robots *Sci. Robot.* **2** eaan4268
[209] Bilodeau R A and Kramer R K 2017 Self-healing and damage resilience for soft robotics: a review *Front. Robot.* AI **4** 48
[210] Galloway K C, Becker K P, Phillips B, Kirby J, Licht S, Tchernov D, Wood R J and Gruber D F 2016 Soft robotic grippers for biological sampling on deep reefs *Soft Robot.* **3** 23–33
[211] Robertson M A, Sadeghi H, Florez J M and Paik J 2017 Soft pneumatic actuator fascicles for high force and reliability *Soft Robot.* **4** 23–32
[212] Wienzek T and Seibel A 2019 Elastomeric prepregs for soft robotics applications *Adv. Eng. Mater.* **21** 1801200
[213] Galley A, Knopf G K and Kashkoush M 2019 Pneumatic Hyperelastic Actuators for Grasping Curved Organic Objects *Actuators* vol **8** p 76
[214] Wakimoto S, Suzumori K and Ogura K 2011 Miniature pneumatic curling rubber actuator generating bidirectional motion with one air-supply tube *Adv. Robot.* **25** 1311–30
[215] Ogura K, Wakimoto S, Suzumori K and Nishioka Y 2009 Micro pneumatic curling actuator-Nematode actuator *2008 IEEE Int. Conf. on Robotics and Biomimetics* (IEEE) pp 462–7
[216] Subramaniam V, Jain S, Agarwal J, Valdivia Y and Alvarado P 2020 Design and characterization of a hybrid soft gripper with active palm pose control *Int. J. Robot. Res.* **39** 1668–85
[217] Goff J, Sulaiman S, Arkles B and Lewicki J P 2016 Soft materials with recoverable shape factors from extreme distortion states *Adv. Mater.* **28** 2393–8
[218] Hassan T Manti M, Passetti G, d'Elia N, Cianchetti M, Laschi C 2015 Design and development of a bio-inspired, underactuated soft gripper *Milan, Italy IEEE Conference Engineering in Medicine and Biology Society (EMBC)* 3619–3622
[219] Hu W and Alici G 2020 Bioinspired three-dimensional-printed helical soft pneumatic actuators and their characterization *Soft Robot.* **7** 267–82
[220] Du Pasquier C, Chen T, Tibbits S and Shea K 2019 Design and computational modeling of a 3D printed pneumatic toolkit for soft robotics *Soft Robot.* **6** 657–63
[221] Chen Y, Xia Z and Zhao Q 2019 Optimal design of soft pneumatic bending actuators subjected to design-dependent pressure loads *IEEE/ASME Trans. Mechatron.* **24** 2873–84
[222] Cho K-J, Koh J-S, Kim S, Chu W-S, Hong Y and Ahn S-H 2009 Review of manufacturing processes for soft biomimetic robots *Int. J. Precis. Eng. Manuf.* **10** 171–81
[223] Alici G, Canty T, Mutlu R, Hu W and Sencadas V 2018 Modeling and experimental evaluation of bending behavior of soft pneumatic actuators made of discrete actuation chambers *Soft Robot.* **5** 24–35
[224] Morin S A, Shepherd R F, Kwok S W, Stokes A A, Nemiroski A and Whitesides G M 2012 Camouflage and display for soft machines *Science* **337** 828–32
[225] Schmitt F, Piccin O, Barbé L and Bayle B 2018 Soft robots manufacturing: a review *Front. Robot.* AI **5** 84
[226] Mutlu R, Tawk C, Alici G and Sariyildiz E 2017 A 3D printed monolithic soft gripper with adjustable stiffness *IECON 2017–43rd Annual Conf. of the IEEE Industrial Electronics Society* (IEEE) pp 6235–40
[227] Peele B N, Wallin T J, Zhao H and Shepherd R F 2015 3D printing antagonistic systems of artificial muscle using projection stereolithography *Bioinspir. Biomim.* **10** 055003
[228] Liravi F and Toyserkani E 2018 Additive manufacturing of silicone structures: a review and prospective *Addit. Manuf.* **24** 232–42
[229] Wallin T J, Pikul J and Shepherd R F 2018 3D printing of soft robotic systems *Nat. Rev. Mater.* **3** 84–100
[230] Gul J Z, Sajid M, Rehman M M, Siddiqui G U, Shah I, Kim K-H, Lee J-W and Choi K H 2018 3D printing for soft robotics–a review *Sci. Technol. Adv. Mater.* **19** 243–62
[231] Shapiro Y, Wolf A and Gabor K 2011 Bi-bellows: pneumatic bending actuator *Sens. Actuators* A **167** 484–94
[232] Shao T, Zhang L, Bao G, Luo X and Yang Q 2014 Basic characteristics of a new flexible pneumatic bending joint *Chin. J. Mech. Eng.* **27** 1143–9
[233] Shintake J, Cacucciolo V, Shea H and Floreano D 2018 Soft biomimetic fish robot made of dielectric elastomer actuators *Soft Robot.* **5** 466–74
[234] de Payrebrune K M and O'Reilly O M 2016 On constitutive relations for a rod-based model of a pneu-net bending actuator *Extreme Mech. Lett.* **8** 38–46
[235] Chirikjian G S and Burdick J W 1994 A modal approach to hyper-redundant manipulator kinematics *IEEE Trans. Robot. Autom.* **10** 343–54
[236] Trivedi D, Lotfi A and Rahn C D 2008 Geometrically exact models for soft robotic manipulators *IEEE Trans. Robot.* **24** 773–80
[237] Polygerinos P, Wang Z, Overvelde J T, Galloway K C, Wood R J, Bertoldi K and Walsh C J 2015 Modeling of soft fiber-reinforced bending actuators *IEEE Trans. Robot.* **31** 778–89
[238] Wang Z and Hirai S 2017 Soft gripper dynamics using a line-segment model with an optimization-based parameter identification method *IEEE Robot. Autom. Lett.* **2** 624–31
[239] Decroly G, Mertens B, Lambert P and Delchambre A 2020 Design, characterization and optimization of a soft fluidic actuator for minimally invasive surgery *Int. J. Comput. Assist. Radiol. Surg.* **15** 333–40
[240] Moseley P, Florez J M, Sonar H A, Agarwal G, Curtin W and Paik J 2016 Modeling, design, and development of soft pneumatic actuators with finite element method *Adv. Eng. Mater.* **18** 978–88
[241] Yeoh O H 1993 Some forms of the strain energy function for rubber *Rubber Chem. Technol.* **66** 754–71
[242] Mooney M 1940 A theory of large elastic deformation *J. Appl. Phys.* **11** 582–92
[243] Ogden R W 1972 Large deformation isotropic elasticity–on the correlation of theory and experiment for

incompressible rubberlike solids *Proc. R. Soc. A* **326** 565–84
[244] Yeoh O H 1990 Characterization of elastic properties of carbon-black-filled rubber vulcanizates *Rubber Chem. Technol.* **63** 792–805
[245] Marechal L, Balland P, Lindenroth L, Petrou F, Kontovounisios C and Bello F 2020 Toward a common framework and database of materials for soft robotics *Soft Robot.* **8** 284–97
[246] Sareh S, Althoefer K, Li M, Noh Y, Tramacere F, Sareh P, Mazzolai B and Kovac M 2017 Anchoring like octopus: biologically inspired soft artificial sucker *J. R. Soc. Interface* **14** 20170395
[247] Low J-H, Ang M H and Yeow C-H 2015 Customizable soft pneumatic finger actuators for hand orthotic and prosthetic applications *2015 IEEE Int. Conf. on Rehabilitation Robotics (ICORR)* (IEEE) pp 380–5
[248] Al-Rubaiai M, Pinto T, Qian C and Tan X 2019 Soft actuators with stiffness and shape modulation using 3D-printed conductive polylactic acid material *Soft Robot.* **6** 318–32
[249] Sparks J L, Vavalle N A, Kasting K E, Long B, Tanaka M L, Sanger P A, Schnell K and Conner-Kerr T A 2015 Use of silicone materials to simulate tissue biomechanics as related to deep tissue injury *Adv. Skin Wound Care* **28** 59–68
[250] Agarwal G, Besuchet N, Audergon B and Paik J 2016 Stretchable materials for robust soft actuators towards assistive wearable devices *Sci. Rep.* **6** 1–8
[251] Martinez R V, Branch J L, Fish C R, Jin L, Shepherd R F, Nunes R M, Suo Z and Whitesides G M 2013 Robotic tentacles with three-dimensional mobility based on flexible elastomers *Adv. Mater.* **25** 205–12
[252] Steck D, Qu J, Kordmahale S B, Tscharnuter D, Muliana A and Kameoka J 2019 Mechanical responses of Ecoflex silicone rubber: compressible and incompressible behaviors *J. Appl. Polym. Sci.* **136** 47025
[253] Runge G, Wiese M, Günther L and Raatz A 2017 A framework for the kinematic modeling of soft material robots combining finite element analysis and piecewise constant curvature kinematics *2017 3rd Int. Conf. on Control, Automation and Robotics (ICCAR)* (IEEE) pp 7–14
[254] Nasab A M, Sabzehzar A, Tatari M, Majidi C and Shan W 2017 A soft gripper with rigidity tunable elastomer strips as ligaments *Soft Robot.* **4** 411–20
[255] Pineda F, Bottausci F, Icard B, Malaquin L and Fouillet Y 2015 Using electrofluidic devices as hyper-elastic strain sensors: experimental and theoretical analysis *Microelectron. Eng.* **144** 27–31
[256] Lee J K, Stoffel N and Fite K 2012 Electronic packaging of sensors for lower limb prosthetics *2012 IEEE 62nd Electronic Components and Technology Conf.* (IEEE) pp 86–91
[257] Byrne O, Coulter F, Glynn M, Jones J F, Ní Annaidh A, O'Cearbhaill E D and Holland D P 2018 Additive manufacture of composite soft pneumatic actuators *Soft Robot.* **5** 726–36
[258] Batsuren K and Yun D 2019 Soft robotic gripper with chambered fingers for performing in-hand manipulation *Appl. Sci.* **9** 2967
[259] Heung K H, Tong R K, Lau A T and Li Z 2019 Robotic glove with soft-elastic composite actuators for assisting activities of daily living *Soft Robot.* **6** 289–304
[260] Zhang Z, Wang X, Liu H, Liang B and Wang S 2018 Kinematic analysis of novel soft robotic arm based on virtual work principle *2018 IEEE Int. Conf. on Robotics and Biomimetics (ROBIO)* (IEEE) pp 984–90
[261] Yang C, Kang R, Branson D T, Chen L and Dai J S 2019 Kinematics and statics of eccentric soft bending actuators with external payloads *Mech. Mach. Theory* **139** 526–41
[262] Wang T, Ge L and Gu G 2018 Programmable design of soft pneu-net actuators with oblique chambers can generate coupled bending and twisting motions *Sens. Actuators* A **271** 131–8
[263] Hu W, Mutlu R, Li W and Alici G 2018 A structural optimisation method for a soft pneumatic actuator *Robotics* **7** 24
[264] Zhang Y, Liu Y, Sui X, Zheng T, Bie D, Wang Y, Zhao J and Zhu Y 2019 A mechatronics-embedded pneumatic soft modular robot powered via single air tube *Appl. Sci.* **9** 2260
[265] Tawk C, Spinks G M, In Het Panhuis M and Alici G 2019 3D printable linear soft vacuum actuators: their modeling, performance quantification and application in soft robotic systems *IEEE/ASME Trans. Mechatron.* **24** 2118–29
[266] Tawk C, Gillett A, In Hetpanhuis M, Spinks G M and Alici G 2019 A 3D-printed omni-purpose soft gripper *IEEE Trans. Robot.* **35** 1268–75
[267] Holzapfel Gerhard - 2000 *Nonlinear solid mechanics II* (Chichester: Wiley)
[268] Allard J, Cotin S, Faure F, Bensoussan P-J, Poyer F, Duriez C, Delingette H and Grisoni L 2007 Sofa-an open source framework for medical simulation *Long Beach, CA, USA* 13-18 *Medicine Meets Virtual Reality*
[269] Payan Y 2012 *Soft Tissue Biomechanical Modeling for Computer Assisted Surgery* vol 11 (Berlin: Springer)
[270] Thieffry M, Kruszewski A, Guerra T-M and Duriez C 2018 Reduced order control of soft robots with guaranteed stability *2018 European Control Conf. (ECC)* (IEEE) pp 635–40
[271] Coevoet E, Morales-Bieze T, Largilliere F, Zhang Z, Thieffry M, Sanz-Lopez M, Carrez B, Marchal D, Goury O and Dequidt J 2017 Software toolkit for modeling, simulation, and control of soft robots *Adv. Robot.* **31** 1208–24
[272] Wu K and Zheng G 2020 Simulation and control co-design methodology for soft robotics *Shenyang, China Chinese Control Conference (CCC)* (https://doi.org/10.23919/CCC50068.2020.9189205)
[273] Sin F S, Schroeder D and Barbič J 2013 Vega: Non-Linear FEM Deformable Object Simulator *Computer Graphics Forum* vol **32** pp 36–48
[274] Sanchez J, Mateo C M, Corrales J A, Bouzgarrou B-C and Mezouar Y 2018 Online shape estimation based on tactile sensing and deformation modeling for robot manipulation *2018 IEEE/RSJ Int. Conf. on Intelligent Robots and Systems (IROS)* (IEEE) pp 504–11
[275] Pozzi M, Miguel E, Deimel R, Malvezzi M, Bickel B, Brock O and Prattichizzo D 2018 Efficient fem-based simulation of soft robots modeled as kinematic chains *2018 IEEE Int. Conf. on Robotics and Automation (ICRA)* (IEEE) pp 1–8
[276] Hiller J and Lipson H 2014 Dynamic simulation of soft multimaterial 3d-printed objects *Soft Robot.* **1** 88–101
[277] Cheney N, MacCurdy R, Clune J and Lipson H 2013 Unshackling evolution: evolving soft robots with multiple materials and a powerful generative encoding *Proc. of the 15th Annual Conf. on Genetic and Evolutionary Computation* pp 167–74
[278] Kriegman S, Cappelle C, Corucci F, Bernatskiy A, Cheney N and Bongard J C 2017 Simulating the evolution of soft and rigid-body robots *Proc. of the Genetic and Evolutionary Computation Conf. Companion* pp 1117–20

[279] Lee K-H, Fu D K, Leong M C, Chow M, Fu H-C, Althoefer K, Sze K Y, Yeung C-K and Kwok K-W 2017 Nonparametric online learning control for soft continuum robot: an enabling technique for effective endoscopic navigation *Soft Robot.* **4** 324–37
[280] Thuruthel T G, Shih B, Laschi C and Tolley M T 2019 Soft robot perception using embedded soft sensors and recurrent neural networks *Sci. Robot.* **4** eaav1488
[281] Giorelli M, Renda F, Calisti M, Arienti A, Ferri G and Laschi C 2015 Learning the inverse kinetics of an octopus-like manipulator in three-dimensional space *Bioinspir. Biomim.* **10** 035006
[282] Li M, Kang R, Branson D T and Dai J S 2017 Model-free control for continuum robots based on an adaptive Kalman filter *IEEE/ASME Trans. Mechatron.* **23** 286–97
[283] Zhang Z, Bieze T M, Dequidt J, Kruszewski A and Duriez C 2017 Visual servoing control of soft robots based on finite element model *2017 IEEE/RSJ Int. Conf. on Intelligent Robots and Systems (IROS)* (IEEE) pp 2895–901
[284] Hyatt P, Kraus D, Sherrod V, Rupert L, Day N and Killpack M D 2018 Configuration estimation for accurate position control of large-scale soft robots *IEEE/ASME Trans. Mechatron.* **24** 88–99
[285] Watanabe T, Yamazaki K and Yokokohji Y 2017 Survey of robotic manipulation studies intending practical applications in real environments-object recognition, soft robot hand, and challenge program and benchmarking *Adv. Robot.* **31** 1114–32
[286] Rosset S and Shea H R 2013 Flexible and stretchable electrodes for dielectric elastomer actuators *Appl. Phys.* A **110** 281–307
[287] Wang C, Sim K, Chen J, Kim H, Rao Z, Li Y, Chen W, Song J, Verduzco R and Yu C 2018 Soft ultrathin electronics innervated adaptive fully soft robots *Adv. Mater.* **30** 1706695
[288] Hu Y, Qi K, Chang L, Liu J, Yang L, Huang M, Wu G, Lu P, Chen W and Wu Y 2019 A bioinspired multi-functional wearable sensor with an integrated light-induced actuator based on an asymmetric graphene composite film *J. Mater. Chem.* C **7** 6879–88
[289] Tabassian R, Nguyen V H, Umrao S, Mahato M, Kim J, Porfiri M and Oh I-K 2019 Graphene mesh for self-sensing ionic soft actuator inspired from mechanoreceptors in human body *Adv. Sci.* **6** 1901711
[290] Sachyani Keneth E, Scalet G, Layani M, Tibi G, Degani A, Auricchio F and Magdassi S 2020 Pre-programmed tri-layer electro-thermal actuators composed of shape memory polymer and carbon nanotubes *Soft Robot.* **7** 123–9
[291] Amjadi M and Sitti M 2018 Self-sensing paper actuators based on graphite–carbon nanotube hybrid films *Adv. Sci.* **5** 1800239
[292] McCoul D, Hu W, Gao M, Mehta V and Pei Q 2016 Recent advances in stretchable and transparent electronic materials *Adv. Electron. Mater.* **2** 1500407
[293] Yang T H, Shintake J, Kanno R, Kao C R and Mizuno J 2020 Low-cost sensor-rich fluidic elastomer actuators embedded with paper electronics *Adv. Intell. Syst.* 2000025
[294] Wang Z and Hirai S 2016 A 3D printed soft gripper integrated with curvature sensor for studying soft grasping *2016 IEEE/SICE Int. Symp. on System Integration (SII)* (IEEE) pp 629–33
[295] Kim D H, Lee S W and Park H-S 2016 Sensor evaluation for soft robotic hand rehabilitation devices *2016 6th IEEE Int. Conf. on Biomedical Robotics and Biomechatronics (Biorob)* (IEEE) pp 1220–3
[296] Robinson S S, O'Brien K W, Zhao H, Peele B N, Larson C M, Mac Murray B C, Van Meerbeek I M, Dunham S N and Shepherd R F 2015 Integrated soft sensors and elastomeric actuators for tactile machines with kinesthetic sense *Extreme Mech. Lett.* **5** 47–53
[297] Zhao H, O'Brien K, Li S and Shepherd R F 2016 Optoelectronically innervated soft prosthetic hand via stretchable optical waveguides *Sci. Robot.* **1** eaai7529
[298] Jung J, Park M, Kim D and Park Y-L 2020 Optically sensorized elastomer air chamber for proprioceptive sensing of soft pneumatic actuators *IEEE Robot. Autom. Lett.* **5** 2333–40
[299] Truby R L, Wehner M, Grosskopf A K, Vogt D M, Uzel S G, Wood R J and Lewis J A 2018 Soft somatosensitive actuators via embedded 3D printing *Adv. Mater.* **30** 1706383
[300] Ozel S, Skorina E H, Luo M, Tao W, Chen F, Pan Y and Onal C D 2016 A composite soft bending actuation module with integrated curvature sensing *2016 IEEE Int. Conf. on Robotics and Automation (ICRA)* (IEEE) pp 4963–8
[301] Tao W, Skorina E H, Chen F, McInnis J, Luo M and Onal C D 2015 Bioinspired design and fabrication principles of reliable fluidic soft actuation modules *2015 IEEE Int. Conf. on Robotics and Biomimetics (ROBIO)* (IEEE) pp 2169–74
[302] Luo M, Skorina E H, Tao W, Chen F, Ozel S, Sun Y and Onal C D 2017 Toward modular soft robotics: proprioceptive curvature sensing and sliding-mode control of soft bidirectional bending modules *Soft Robot.* **4** 117–25
[303] Ozel S, Keskin N A, Khea D and Onal C D 2015 A precise embedded curvature sensor module for soft-bodied robots *Sens. Actuators* A **236** 349–56